Conducting and Magnetic Langmuir–Blodgett Films

Daniel R. Talham*

Department of Chemistry, University of Florida, P.O. Box 117200, Gainesville, Florida 32611-7200

Received April 13, 2004

Contents

Daniel R. Talham is currently Professor of Chemistry at the University of Florida. His research interests include the fabrication of thin films and understanding of interfaces in mixed organic/inorganic materials. Themes include conductivity and magnetism in low-dimensional systems, biominerals, and biomaterials. He grew up in New York state and performed undergraduate and graduate studies at The Johns Hopkins University, receiving his Ph.D. in 1985 under the supervision of Prof. Dwaine O. Cowan. He then moved to England for postdoctoral studies at Oxford University's Inorganic Chemistry Laboratory with Prof. Peter Day. As part of this stay in Europe, he spent 6 months at the Laboratoire de Physique des Solides, Université Paris-Sud, working with Dr. Patrick Batail. In 1987, he returned to the U.S. for a postdoctoral appointment with Prof. Mark S. Wrighton at MIT. He began his appointment at the University of Florida as an Assistant Professor in 1989.

1. Introduction

An underlying principle of molecule-based conductors is that cooperative properties depend on intermolecular interactions and, therefore, the arrangement of molecules in condensed phases. Electronic band structures are determined by the distances between molecules and their orientation relative to each other. The same basis molecule in the same oxidation state can lead to dramatically varied solid-state properties if it crystallizes in different phases involving different molecular packing configurations. This point was hammered home in the early days of studies on the organic donor bis(ethylenedithio)-tetrathiafulvalene (BEDT-TTF), **1**, which, in cation-

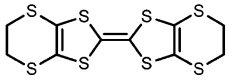

BEDT-TTF **1**

radical salts of the same counterion, can form multiple polymorphs with electronic properties that range from insulator to semiconductor to metal to superconductor.[1–3] The same principle applies to the design and synthesis of molecule-based magnets. Cooperative magnetism depends on the interaction between magnetic sites, which, in turn, depends on factors such as intersite distance, relative orientation, and electronic overlap with groups that link them.[4]

Research in both fields began by focusing on molecular properties and the issue of solid-state behavior was left to the vagaries of crystallization. Ultimately, "design constraints" began to invoke crystal engineering and supramolecular assembly

* To whom correspondence should be addressed. E-mail: talham@chem.ufl.edu. Tel.: 352 392 9016. Fax: 352 392 3255.

10.1021/cr030665u CCC: $48.50
Published on Web 10/23/2004

concepts.[3–6] Nevertheless, despite significantly greater understanding of the factors that dictate molecular packing, our ability to design a functional molecule and predict how it will arrange in the solid state is quite limited. The problem is exacerbated as molecular features that influence the targeted cooperative phenomena, such as delocalized π-systems and donor/acceptor character, also contribute to crystal packing forces. The problems of the electronic or magnetic structure of the molecular building blocks cannot be separated from solid-state engineering.

The Langmuir−Blodgett (LB) method organizes a single layer of molecules on a liquid surface, usually water, before transfer to a solid support to form a thin film with the thickness of a constituent molecule.[7–10] Two factors have attracted researchers to studies of LB films of molecule-based conductors and magnets. First is the ability to process the molecules and form thin films, which are preferred over small crystalline samples for many applications. Second, LB films are perhaps the earliest examples of supramolecular assembly, providing the opportunity to exercise molecular-level control over the structure of the films. Although the LB method does not solve all problems associated with engineering the structure of condensed phases, it does provide a level of control over the orientation and placement of molecules in monolayer and multilayer assemblies that is not otherwise available.

Studies of LB films of molecular conductors date back to the mid 1980s.[11,12] Several reviews of the topic have been published,[13–17] the most recent in 2001. Magnetism in LB films dates back even further, to the late 1970s.[18–20] This topic has not been comprehensively reviewed, although a book chapter on magnetic LB films appeared recently.[21] In the present article, the literature on LB films of molecular conductors is reviewed back to 1999, overlapping somewhat with a previous review,[17] although earlier work that helped define different approaches to conducting films is also included. This review does not address the literature on LB films of conducting or electroactive polymers or the use of LB methods to organize nanoparticles. The subject of electroactive polymers in LB films was included in an earlier review by Nakamura.[15] Also, the topic of molecular rectifiers, many of which have been studied in LB films, was reviewed by Metzger in the past year[22] and so is not covered here. The literature on magnetic LB films is reviewed starting from 1995, but again, earlier work that set the stage for recent studies is described. I have tried to be comprehensive, and any omissions are oversights on my part and are not intentional.

Finally, control over layer-by-layer deposition and molecular orientation has led researchers to use the LB platform in attempts to combine properties in a single assembly, to form hybrid materials[23] or "dual-network" assemblies[24] such as photocondutors, photomagnets, or magnetic conductors (Figure 1). The literature on these efforts is also included. The review begins with a brief introduction to LB films.

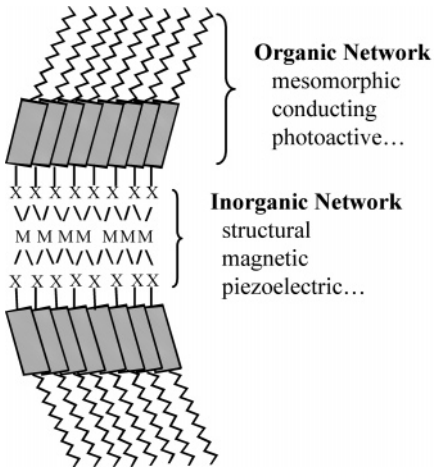

Figure 1. Scheme of a dual-network LB film with a molecular solid organic network and an inorganic extended lattice network. One of the promises of LB films is the ability to mix properties attributable to different types of matter within a single assembly.

2. Langmuir–Blodgett Films[7–10]

The layer of molecules on a liquid surface is termed a *Langmuir monolayer*, and after transfer, it is called a *Langmuir−Blodgett film*. The technique is named after Irving Langmuir and Katharine Blodgett, researchers at the General Electric Company in the first half of the 20th century. Langmuir, awarded the Nobel Prize for Chemistry in 1932 for his studies of surface chemistry, used floating monolayers to learn about the nature of intermolecular forces. Working principally with fatty acids, Katharine Blodgett, together with Langmuir, refined the method of transferring the floating monolayer onto solid supports.[25] Much of the current interest in LB films derives inspiration from the pioneering work of Hans Kuhn in the 1960s who used LB methods to control the position and orientation of functional molecules within complex assemblies,[26] an elegant early example of what is currently being called "supramolecular assembly." To acknowledge Kuhn's contributions, some authors now term transferred films of functional molecules Langmuir−Blodgett−Kuhn (LBK) films.

2.1. Langmuir Monolayers

Essentially all LB film work begins with the Langmuir−Blodgett trough containing an aqueous subphase (Figure 2). Moveable barriers that can skim the surface of the subphase permit control of the surface area available to the floating monolayer. To form a Langmuir monolayer, the molecule of interest is dissolved in a volatile organic solvent (frequently chloroform or hexane) that will not react with or dissolve into the subphase. Surface-active molecules are normally amphiphilic, with separate polar and hydrophobic groups, like the fatty acids studied by Langmuir and Blodgett. A quantity of this solution is placed on the surface of the subphase, and as the solvent evaporates, the surfactant molecules spread. Generally, the state of the monolayer on the water surface is monitored by measuring the surface pressure, defined as the difference between the surface

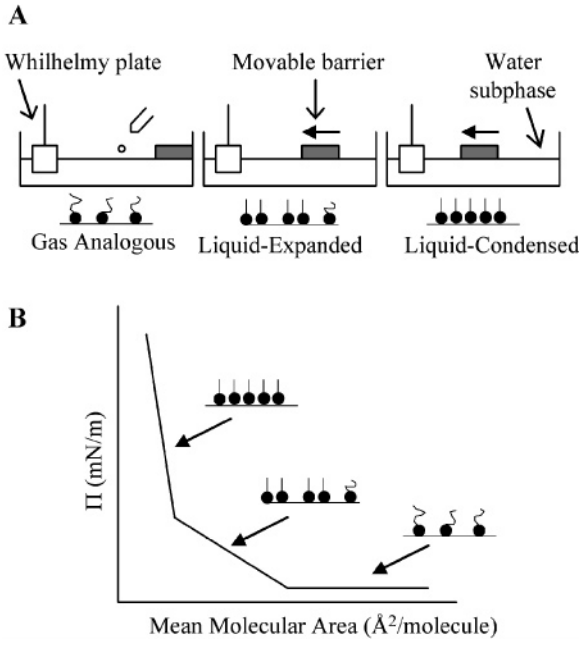

Figure 2. Compression of a Langmuir monolayer. (A) Scheme of a Langmuir–Blodgett trough as the moveable barrier reduces the area available to the monolayer. (B) Idealized pressure vs area isotherm indicating phase transitions of the monolayer.

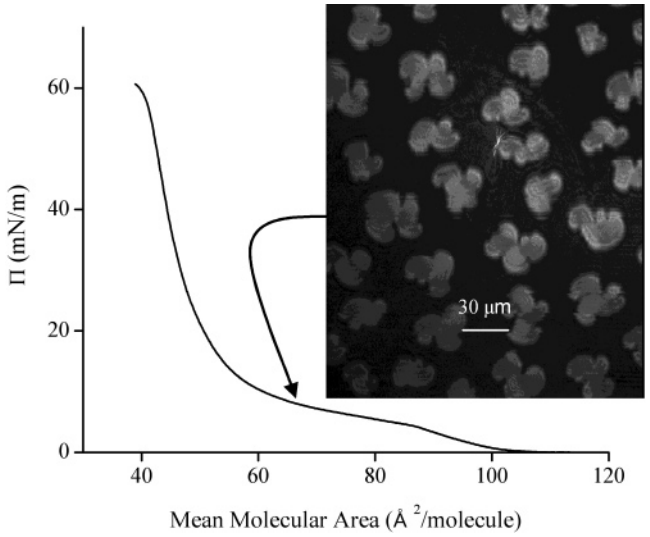

Figure 3. Pressure vs area isotherm and Brewster angle microscopy image of a monolayer of DPPC. The BAM image shows the coexistence of two phases, taken during the transition from the liquid-expanded phase (dark features) to the liquid-condensed phase (lighter features).

tension of the monolayer (γ) and the pure subphase (γ_0), $\Pi = \gamma_0 - \gamma$.

An idealized pressure vs area isotherm is included in Figure 2. As the pressure increases, the two-dimensional monolayer goes through different phases that have some analogy with the three-dimensional gas, liquid, and solid states. If the area per molecule is sufficiently high, then the floating film will be in a two-dimensional gas phase where the surfactant molecules are not interacting. As the monolayer is compressed, the pressure rises, signaling a change in phase to a two-dimensional liquid-expanded (LE) state, which is analogous to a three-dimensional liquid. Upon further compression, the pressure begins to rise more steeply as the liquid-expanded phase gives way to a condensed phase (or a series of condensed phases). This transition, analogous to a liquid–solid transition in three dimensions, does not always result in a true two-dimensional solid. Rather, condensed phases tend to have short-range structural coherence and are called liquid-condensed (LC) phases. As the pressure is increased further, the monolayer will eventually collapse under the pressure, either sliding over upon itself or folding under into the subphase. When two phases are in equilibrium, such as gas and LE phases, or LE and LC, the surface pressure will plateau over a range of mean molecular area. An image recorded by the author's group of two phases in equilibrium is shown in Figure 3. The example is the extensively studied phospholipid DPPC (1,2-dipalmitoyl-*sn*-glycero-3-phosphatidylcholine)[27] in equilibrium between LE and LC phases.

By extrapolating the steepest part of the curve prior to collapse to zero pressure, a minimum cross-sectional area per molecule can be found. However, an isotherm alone is not sufficient to determine whether a molecule forms a monolayer. There are many examples of "reasonable" isotherms that correspond to multilayers or films that have not completely spread. Monolayer behavior should be confirmed with complementary methods such as surface potential measurements, fluorescence microscopy, Brewster angle microscopy, or X-ray or neutron reflectivity or diffraction. In addition, isotherms also change as a function of temperature. At any given temperature, the monolayer might pass through several phases during compression or only a couple.

2.2. Langmuir–Blodgett Films

The term "Langmuir–Blodgett film" traditionally refers to monolayers that have been vertically transferred off the water subphase and onto a solid support such as glass, silicon, mica, or quartz. Vertical deposition is the most common method of LB transfer; however, horizontal lifting of Langmuir monolayers onto solid supports, called Langmuir–Schaeffer deposition, is also possible.

Either highly hydrophilic or highly hydrophobic substrates are desired. When hydrophobic, the substrate originates above the water surface. After the monolayer has been spread and compressed to the desired transfer pressure, the substrate is dipped vertically through the monolayer with transfer via the hydrophobic interactions between the alkyl chains and the surface. A hydrophilic substrate is submerged in the aqueous subphase prior to the spreading and compressing of the monolayer film. After the monolayer has stabilized, the substrate is withdrawn from the subphase, and the hydrophilic interactions drive the transfer (Figure 4).

Different film architectures can result upon deposition (Figure 4b). Y-type multilayers are most common and can be prepared on either hydrophilic or hydrophobic substrates. They are typically the most stable because of the strength of the head–head and tail–tail interactions. X-type and Z-type films are rare. In fact, with some amphiphiles, even when films have

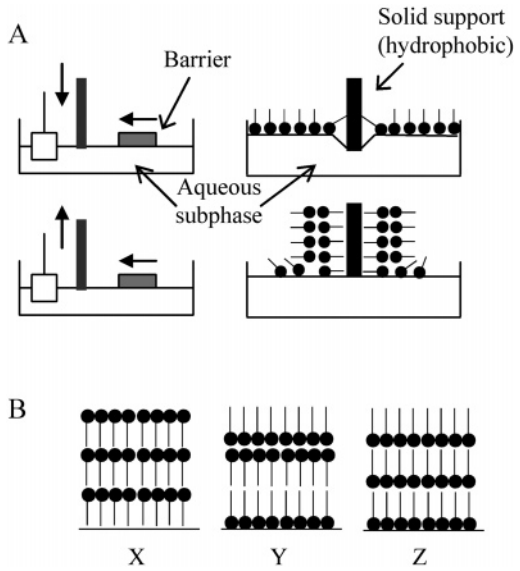

Figure 4. (A) Langmuir−Blodgett deposition starting with a hydrophobic substrate. (B) Possible film architectures in idealized Langmuir−Blodgett films.

been deliberately transferred by an X- or Z-method, the spacing between the hydrophilic headgroups shows packing similar to that of Y-type films, implying that some molecular rearrangement occurs during or shortly after deposition.

2.2.1. Characterization of Transferred Films

Many analytical techniques are used to study transferred films. In addition to the material properties, discussed later, film characteristics that are typically of interest are thickness, interlayer spacing, molecular orientation and packing, film coverage, surface topology, and chemical composition. The techniques used to study these parameters are well described in textbooks on LB films.[7−10]

X-ray diffraction is a reliable technique to probe interlayer spacing, and from interlayer spacing, film thickness can be inferred. However, even X-ray diffraction is not proof that an LB film transfers as uniform layers. Many amphiphiles, when condensed, will do so with a layered structure that will look the same in X-ray diffraction as a well-organized LB film. Some measure of the uniformity of the film should complement X-ray diffraction. Film thickness can also be determined by ellipsometry or X-ray or neutron reflectivity. Grazing-incidence X-ray diffraction (GIXD) is a method for determining the arrangement of molecules within a floating Langmuir monolayer.[28] The same methods can be applied to transferred films, but this is more difficult because solid supports are not as flat as the surface of water. Transmission electron diffraction has also been observed from LB films and used to determine molecular packing, although organic films are mostly unstable to the electron beam. Atomic force microscopy (AFM) with molecular-scale resolution has also been used to observe the arrangement of molecules in transferred monolayer and multilayer films.[29]

To study the chemical makeup of the films, standard spectroscopic methods can be used, including FTIR spectroscopy, Raman scattering, and UV−visible absorption.[13] These methods are often sensitive enough to be applied to even monolayer films. Solid-state NMR spectroscopy has also been applied to LB films but is complicated by the small amount of materials available, so such studies are not routine.[30] The elemental composition can be determined with X-ray photoelectron spectroscopy (XPS).[31,32] However, the intensities of the XPS peaks are sensitive to many parameters such as an element's electron escape depth and the film geometry, factors that complicate the determination of the elemental ratios.

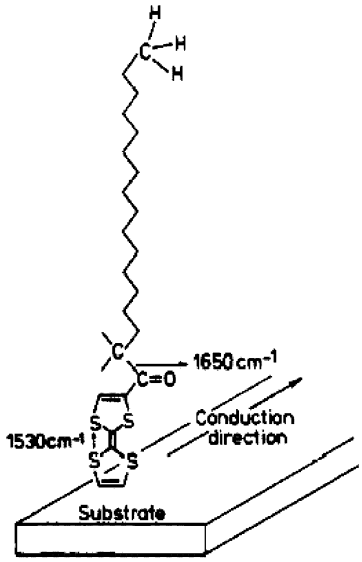

Figure 5. Orientation of HDTTF, **6**, relative to the substrate after transfer and doping (adapted from ref 33).

3. LB Films of Molecular Conductors

Routes to the formation of conducting LB films generally involve molecular building blocks similar to those used in the pursuit of conducting molecular solids, principally tetrathiafulvalene (TTF) (**2**) family donors, tetracyanoquinodimethane (TCNQ) (**3**) family acceptors, metal dithiolate complexes (**4**), and phthalocyanines (**5**). To form monolayers at the air/water interface, the molecular-basis molecules must be included in an amphiphilic assembly, and this has been accomplished in a couple of ways. One approach is to substitute the basis molecule to make it amphiphilic, by adding hydrophobic groups, as in the substituted TTF **6**[33] (Figure 5), or by substituting with both hydrophobic and hydrophilic groups, as in

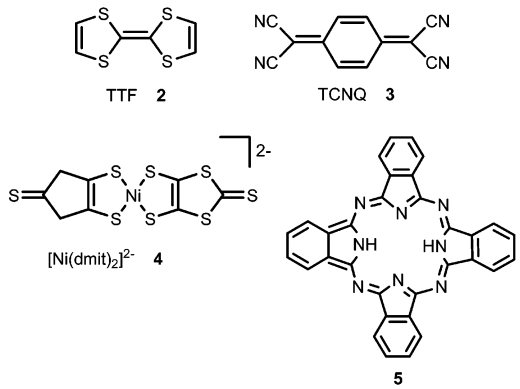

the TTF derivative **7**.[34] Another approach, sometimes called the "semiamphiphilic approach",[13] is to associate the nonamphiphilic active molecule with an amphiphilic counterion, as for the pyridinium TCNQ salt *N*-docosylpyridinium TCNQ (**8**).[11,35]

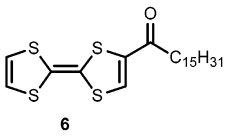

6

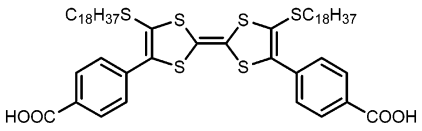

7

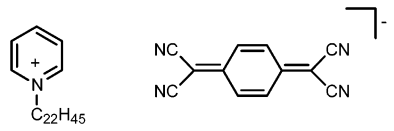

8

For either of these approaches, the resulting films often comprise either neutral or fully charge-transferred basis molecules, and subsequent treatment to achieve mixed valency is required to form conducting films. The most common route to doped films is postdeposition chemical treatment, for example, with a vapor-phase oxidant such as I_2.[33,35] Although oxidation is normally achieved, films are sometimes unstable to charge back-transfer and outgassing of the dopant. Electrochemical oxidation or reduction of the film during or after deposition onto an electrode surface or array is also possible.[13,15] Another way to achieve mixed valency is to start with a mixture of neutral and charged basis molecules to give an average oxidation state in the final assembly.[36] Alternatively, the film can be a traditional charge-transfer salt, comprising donors and acceptors, one or both of which have been substituted to be amphiphilic.[37]

Recent developments in the area of molecular-conductor-based Langmuir–Blodgett films, surveyed back to 1999, are presented in the next subsections. The presentation is organized according to the nature of the basis molecule involved. Methods used to prepare films and achieve mixed valency differ but are largely variations of the methods just described. Much of the recent work in this area builds on previous efforts, dating back to the mid 1980s. Although all of this early literature is not reviewed here, examples have been chosen that helped define a class of molecular-basis molecules or a route to forming the conducting film. Recent developments are then included within the context of these early examples. Previous review articles should be consulted for a more complete survey of work before 1999.[13–17]

Emphasis here is on the identity of the basis molecules; the methods used to form films of each example; and the result, whether it is conducting or not. In some cases, descriptions of the structure of the resulting film will be provided, if known. Details of the structural and spectroscopic methods used to reach the conclusions reported in a given paper will not be presented. Methods used for structural characterization of LB films[8–10] and the spectroscopic and transport measurements used to understand the electronic properties of conducting LB films have been reviewed[13] and so will not be repeated here. However, the reader should keep in mind that studies of LB films normally require combinations of multiple techniques to develop a coherent picture of the physical structure, electronic structure, or magnetic structure of the thin film. By including work in this review, I do not imply that unambiguous structural and physical properties analyses have been carried out. I have not scrutinized each work for completeness. For this, readers are directed to the original literature.

3.1. LB Films Based on TCNQ

Raudel-Teixier, Vandevyver, and Barraud prepared the first examples of conductive LB films using *N*-docosylpyridinium TCNQ (**8**).[12] Upon LB film transfer, the TCNQ is anionic, so subsequent oxidation with iodine vapor was used to achieve mixed valency. These authors, along with Nakamura and co-workers, mapped out the use of a combination of analytical methods to learn about the structure of conducting LB films.[11,12,35,38] X-ray diffraction combined with UV–visible, IR, and EPR spectroscopies were used to establish that, in the precursor film, $(TCNQ^-)_2$ dimers are oriented with their molecular planes parallel to the substrate surface, but upon partial oxidation, the TCNQ moieties reorient to align the long molecular axis perpendicular to the substrate.

The conductivity after treatment was 0.1 S cm^{-1} with an activation energy of 0.15 eV. However, the film had a domain structure, with less-organized grain boundaries separating the more highly conducting domains. Therefore, the measured conductivity was less than the intrinsic conductivity, estimated to be as high as 200 S cm^{-1} from optical measurements. This feature of the macroscopic conductivity being limited by domain structure and film imperfections has turned out to be a common characteristic of conducting LB films.[15,16]

Recent work that follows this approach includes a charge-transfer complex of TCNQ and the amphiphilic cation *N*-octadecylbenzidine that was first prepared and spread at the air/water interface before being transferred as an LB film.[39] Postdeposition iodine doping increased conductivity by 2 orders of magnitude, reaching a maximum value of 4×10^{-4} S cm^{-1}. Similarly, TCNQ can be incorporated at positively charged monolayers from a LiTCNQ aqueous subphase, as exemplified with a diphenylbis(octadecylamino)phosphonium ion ($DPOP^+$) Langmuir monolayer.[40] In a variation on pyridinium TCNQ films, an azobenzene moiety (**9**) has been

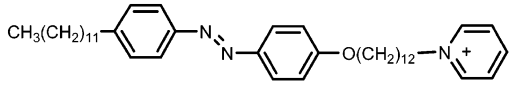

9

incorporated into the alkyl tail of the amphiphilic pyridinium counterion. Irradiation of a film of the TCNQ salt of **9** at frequencies that induce trans-to-cis isomerization of the azobenzene results in changes in the in-plane conductivity.[41]

3.1.1. TCNQ Amphiphiles

Raudel-Teixier, Vandevyver, and Barraud also prepared LB films of an amphiphilic TCNQ (C_n-TCNQ, **10**).[36] One approach to achieve mixed valency

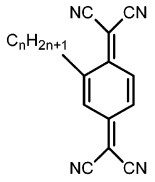

n = 14, 16, 22

10

with this system is to mix the neutral TCNQ amphiphile with fully reduced $TCNQ^-$ as the salt of a cationic surfactant.[42] The mixed monolayers are stable, and conductivities in transferred films of 0.1 S cm^{-1} have been observed, for example, in multilayer films of [octadecyldimethylsulfonium][(C_nTCNQ)-(TCNQ)]. The mixed-valency film is also characterized by the presence of an intermolecular charge-transfer band in the IR spectrum.

An LB analogue of the organic/inorganic coordination polymer CuDCNQI has been studied.[43−45] Monolayers of the amphiphile 2-methyl-5-octadecylDCNQI, **11**, have been prepared with and without added

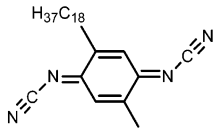

11

CuI. Optical spectroscopy of the floating monolayer indicates that the acceptor is neutral at the air/water interface, even in the presence of copper ion. Upon transfer, however, the DCNQI amphiphile is fully reduced. The full charge transfer ($\rho = 1$) is different from that observed for the crystalline parent complex, $Cu(DMeDCNQI)_2$, for which $\rho = {}^2/_3$.

3.1.2. Charge-Transfer Salts of TCNQ Amphiphiles

TCNQ amphiphiles can also form charge-transfer salts with traditional donors, and some examples have resulted in very high conductivity films. The C_n-TCNQ complex with BEDO-TTF, **12**, forms stable

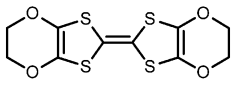

BEDO-TTF **12**

films when mixed with an inert cosurfactant such as icosanoic acid.[15,46,47] The conductivity of the monolayer at the air/water interface has been measured as 0.6 S cm^{-1}. Transferred films have even higher conductivity and were shown to be metallic by Hall measurements, EPR spectroscopy, and temperature-dependent conductivity. The LB films are deposited using horizontal dipping methods.

3.2. Amphiphilic TTF Derivatives

The amphiphile EDT-TTF$(SC_{18})_2$ (**13**), with two hydrophobic chains, has been studied in detail.[13,48−50]

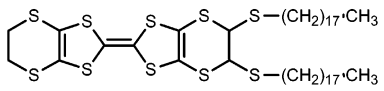

13

To form a stable monolayer, the donor must be mixed with traditional fatty acids. A mixed-valency film is generated after transfer by reaction with iodine vapor. The complex oxidation process has been mapped out whereby initial reaction completely oxidized the donor molecules in the film, but upon waiting or purposeful annealing, a mixed-valent state is generated accompanied by significant reorganization of the film. Spectroscopic analysis suggests that a mixed-valent triiodide salt results, [EDT-TTF-$(SC_{18})_2]_2I_3$. Conductivity up to 1 S cm^{-1} is observed for multilayer films, although for films of only a few layers, the dc conductivity disappears. Analysis of the charge-transfer bands in the IR absorption spectra indicates an even higher intrinsic conductivity than that determined by dc measurements. The evidence suggests a percolation model for the conductivity. Multilayer films were studied with varying percentages of fatty acid cosurfactant, and the results support the model of a heterogeneous mixed film of conducting [EDT-TTF$(SC_{18})_2]_2I_3$ clusters surrounded by nonconducting fatty acid bilayers.

The amphiphilic TTF derivatives HDTTF (**6**) and HDTTTF (**15**) illustrate the idea of modifying a TTF

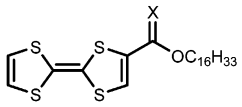

X = O **14**

X = S **15**

donor to generate film-forming amphiphiles.[14,33,51] The neutral amphiphiles spread on water and can be deposited onto a variety of substrates as Y-type films using normal dipping procedures. Chemical oxidation after deposition is required to form a charge-transfer salt, and iodine vapor oxidation has been the most successful approach. As for salts of **13**, initial exposure to iodine generates fully oxidized TTF cations, but the film gradually releases iodine to stabilize in a mixed-valent conducting state. The films also reorganize after doping and apparently interdigitate. IR and optical measurements suggest a nearly vertical orientation of the amphiphile after doping with respect to the solid support surface (Figure 5). The conductivity of the oxidized thiocarboxy analogue is the highest in the series. The two-probe dc conductivity was measured as 1.0 ± 0.2 S cm^{-1} with an activation energy of 0.09 eV. Again, this conductivity is high for an LB film, but low compared to those of related solid-state charge-transfer salts.

New tetrathiafulvalene donors containing pyridine groups (**16**, **17**), but without long alkyl groups, were

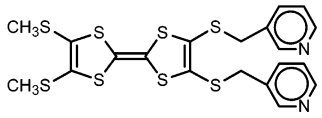

16

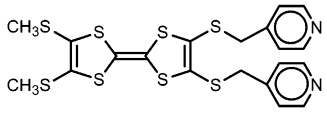

17

reported to form Langmuir monolayers with and without the presence of silver ion in the subphase.[52,53] Multilayer LB films were deposited and subsequently oxidized with iodine vapor to give stable charge-transfer salts. Conductivities, measured by two-probe techniques, were shown to increase from $\sim 10^{-7}$ to $\sim 10^{-3}$ S·cm^{-1} upon iodine oxidation.

The same group has prepared new BEDT-TTF derivatives containing hydroxyl groups and long alkyl chains (**18**, **19**) and studied them alone as Langmuir

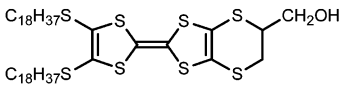

18

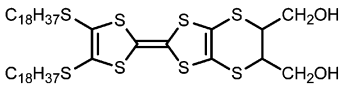

19

monolayers and as mixtures with arachidic acid.[54] Postdeposition iodine doping yielded cation-radical salts but small changes in conductivity. The poor conductivities were attributed to the formation of a domain structure that is discontinuous.

A series of electrically active LB films based on the amphiphilic monopyrrolotetrathiafulvalene donor (**20**)

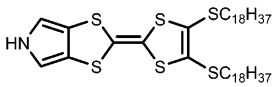

20

have been investigated as charge-transfer salts with different TCNQ aceptors, including the parent TCNQ, monofluoro, 2,5-difluoro, 2,5-dimethyl, 2-methoxy-5-ethoxy, and 2-decyl derivatives.[55] The degree of charge transfer varied depending on the acceptor, resulting in electronic ground states that ranged from neutral to fully ionic. Of the complexes that were studied, those with TCNQ and the amphiphilic decyl-TCNQ acceptors gave films with partial charge transfer.

In another effort to switch conductivity in molecular-conductor LB films, Bryce and co-workers coupled an azobenzene chromophore to TTF (**21**).[56] Semiconducting LB films were formed without the need for a fatty acid cosurfactant. However, no change in conductivity was observed upon illumination. If the condensed phase is too well organized, then trans-to-cis isomerization will be hindered, and that appears to have happened here.

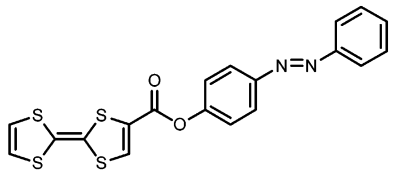

21

The compound 4-ethoxycarbonyl-4′,5,5′-trimethyltetrathiafulvalene (**22**) undergoes intramolecular

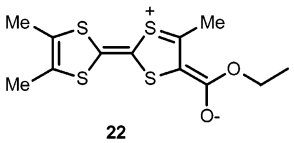

22

charge transfer from the TTF donor to the ethoxycarbonyl acceptor, forming a zwitterion that is reported to spread as a Langmuir monolayer without the need for added fatty acid.[57] The monolayers could be transferred as LB films. The in-plane conductivity of the as-transferred film is approximately 10^{-5} S cm^{-1}. Postdeposition oxidation with iodine vapor generates the radical cation, and the in-plane conductivity rises to 10^{-1} S cm^{-1} with an activation energy of 0.11 eV. LB films of the compound are electrochemically active, and two quasi-reversible oxidation waves are observed for films of two layers. For thicker films, the cyclic voltamogram becomes distorted, most likely because of limited counterion diffusion through the film. Although the film conductivity increases upon postdeposition electrochemical oxidation, it is to a lesser extent than when the film is treated with I_2 vapor. Spectroscopic analysis of the neutral and iodine-treated films indicates a highly anisotropic film with the TTF units aligned and oriented at a high angle with respect to the substrate surface. The compound provides an example of a single-component TTF derivative without a traditional hydrophobic tail that can be used to form highly conducting LB films.

Bryce and co-workers also recently reported a film-forming covalent TTF-TCNQ diad (**23**) of the type

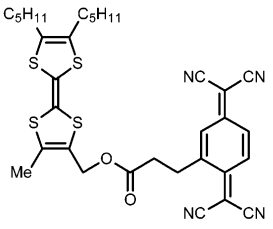

23

normally targeted as potential molecular rectifiers.[58] The compound has a low electrochemical HOMO–LUMO gap of 0.17 eV. Intramolecular charge transfer is observed in solutions of the compound. Detailed studies of attempts to observe rectification in monolayers have not yet been published, but multilayer films are described and in-plane conductivities were measured for both neutral and iodine-vapor-treated

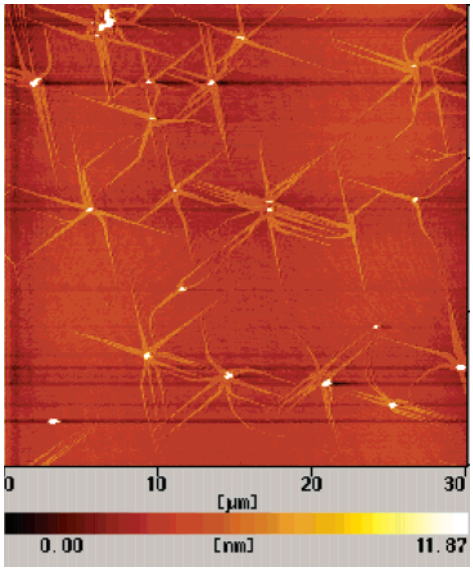

Figure 6. AFM (30 × 30 μm^2) image of the nanowires formed from compound **24** deposited on mica by the horizontal lifting method from a 0.01 M KCl aqueous solution. (Adapted with permission from ref 60. Copyright 2002, National Academy of Sciences, U.S.A.)

films. The neutral film shows no evidence for charge transfer, suggesting that the molecular conformation in the condensed state prohibits interactions between the donor and acceptor fragments. Conductivities are less than 10^{-7} S cm^{-1}. Also, the film does not appear to react with iodine vapor. Although the films have not yielded useful electronic behavior, the paper demonstrates a strategy for preparing TTF-TCNQ diads.

LB films of an amphiphilic bis-tetrathiafulvalene-substituted macrocyclic polyether (**24**) complexed

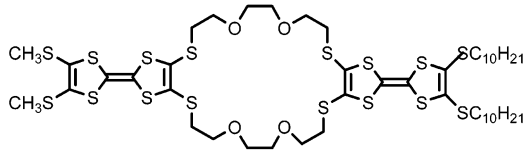

24

with $TCNQF_4$ or $TCNQCl_2$ do not form continuous layered films, but rather rearrange upon transfer to form nanowire structures.[59–61] When deposited onto mica, the nanowires orient according to the hexagonal symmetry of the cleaved mica surface (Figure 6). The films are prepared by mixing the bis-TTF donor and the acceptor in the spreading solvent, forming the charge-transfer complex in solution before spreading. Optical and IR spectroscopy of the transferred nanowires indicates full charge transfer to the $TCNQF_4$ or $TCNQCl_2$ acceptors. If weaker acceptors are used, such as $TCNQF_2$ or TCNQF, the charge-transfer complex does not form at the air/water interface, and the transferred film contains only the bis-TTF donor.[61]

The nanowires are observed upon deposition with either horizontal or vertical dipping methods and represent a reorganization of the monolayer during film transfer. The nanowires have typical widths of 50 nm and can be as long as several microns. The height is typically 2.5 nm. Considering the size of the bis-TTF donor, the wires are composed of 20–30 molecules in width and 1–3 molecules in height. The longitudinal direction of the wires corresponds to the stacking direction of the TTF and acceptor molecules.

The macrocyclic polyether part of the donor can complex metal ions, and the presence of subphase ions is an important variable. Nanowire structures are observed with several subphase metal ions, as well as without them. However, the directionality of the wires, reflecting interactions with the mica surface structure, is strongly influenced by the subphase ions. Straight wires along symmetry directions of the mica are formed with K^+ and to a lesser extent with Rb^+ and Cs^+. The wires grow along the [100], [210], and [$\bar{2}$10] directions of the mica. The authors speculate that the metal ions occupy interlayer K^+ vacancies created upon cleavage of the mica surface. The ions K^+ and Rb^+ provide the best size match with the vacancies, so wires with these ions are longer and the orientations better defined. The directionality is lost completely with Ba^{2+} or with a pure water subphase, and spiral-like structures are formed.[60]

3.3. LB Films Based on Metal Dithiolate Complexes

Metal dithiolate complexes represent another family of building blocks of molecular conductors that have been explored in LB films.[13–16] Principally studied have been Ni^{2+}, Pd^{2+}, Pt^{2+}, and Au^{3+} complexes of the dmit (1,3-dithiole-2-thione-4,5-dithiolate) ligand. In the solid state, a $Ni(dmit)_2$ (**4**) charge-transfer salt with TTF is a superconductor,[62] as are some salts with closed-shell cations.[63] In LB films, metal–dmit complexes have been most extensively studied as salts of alkylammonium or alkylpyridinium amphiphiles.[15,64–66] Typically, the monovalent salts can be spread at the air/water interface with the aid of a cosurfactant such as arachidic acid and transferred as LB films. In some cases, the divalent salts can be spread and transferred without the need of cosurfactant.[67] The partial charge-transfer state is achieved through further oxidation after deposition either with Br_2 or I_2 vapor or through electrochemical treatment in $LiClO_4$ electrolyte.[15]

Several examples have high conductivity, including the bromine-doped film of [didecyldimethylammonium][$Ni(dmit)_2$]. The highest room-temperature conductivities, up to 40 S cm^{-1}, have been reported for a series of trialkylmethylammonium salts of $Au(dmit)_2$.[15] The tridecylmethylammonium analogue has a metallic temperature dependence of the conductivity down to 200 K.[15,65] Below this temperature, the conductivity becomes activated.

Miura and co-workers[68–70] have published a series of papers claiming possible ac susceptibility evidence of superconductivity in ditetradecyldimethylammonium $Au(dmit)_2$ films that have been electrochemically oxidized in the presence of $LiClO_4$. The properties of deposited films of alkylammonium $Au(dmit)_2$ salts have also been investigated as a function of the "waiting time" on the water subphase before compression and transfer.[71–73] Variations in conductivity and IR spectroscopy suggest that significant reorganization and chemical composition change can take

place in the Langmuir monolayer upon resting up to 3 h on the water surface. LB films of [*N*-hexadecylpyridinium][Cd(dmit)$_2$] have also been studied.[74] Exceptional conductivities are reported in both neutral and iodine-doped films, although the reason for the high conductivity is not explained.

Another gold dithiolate complex, bis[bis(methylthio)tetrathiafulvalenedithiolate]gold(III) (**25**), has

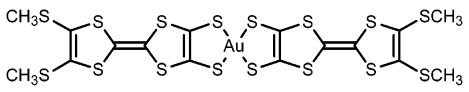

25

been studied in an LB film as a possible single-component conductor.[75,76] Such systems exhibit a small HOMO–LUMO gap, and in the case of significant intermolecular interactions, the bandwidth can overcome the gap to yield a conductor without the need of an external oxidant or reductant. To attempt to form LB films, compound **25** was spread as the monoanion with the tridecylmethylammonium counterion. Upon deposition, the gold dithiolate was oxidized, and the counterion dissolved away to leave the neutral single-component film. The neutral film was poorly conducting, but subsequent electrochemical oxidation in $LiClO_4$ aqueous solution yielded conducting behavior (ca. 1 S cm^{-1}). The treated film exhibited semiconducting behavior down to 110 K with an activation energy of 0.05 eV.

3.4. Films Based on BEDO-TTF

Metallic LB films have also been fabricated based on the donor BEDO-TTF (**12**) that forms monolayers as the cation radical salt of behenate or stearate amphiphiles.[17,77,78] Macroscopic dc conductivities up to 100 S cm^{-1} have been measured, and the temperature dependence of the conductivity is that of a metal to below 150 K. The preparation is one of the simplest for a conducting LB film and, at the same time, represents the most clear-cut example of a conducting molecule-based LB film.

To form the films, BEDO-TTF and the fatty acid are spread together from chloroform at the air/water interface.[77] Partial oxidation of BEDO-TTF occurs spontaneously, and the donors associate with the carboxylate ions that are confined to the air/water interface. There is speculation that the oxidation is proton assisted, but the exact mechanism of cation radical formation is still unclear. Nevertheless, the BEDO-TTF is partially oxidized and organized at the air/water interface, and this assembly can be transferred by normal vertical dipping procedures to obtain multilayered Y-type LB films. The fabrication process is simple relative to other approaches that require synthetic modification of donor or acceptor molecules. In addition, the transferred film is already in a mixed-valent conducting state, so no postdeposition treatment of the films is required.

Infrared reflection–absorption spectroscopy at the air/water interface indicates that the monolayer assembly is already conducting.[77] A broad electronic absorption band in the IR region can be treated with the Drude model to yield an optical conductivity of $\sigma_{opt} \approx 200$ S cm^{-1} for the monolayer. Upon transfer, multilayers assume a bilayer structure. A model for the structure that is consistent with X-ray diffraction, EPR data, and IR spectroscopy consists of BEDO-TTF bilayers organized in a sheet, sandwiched between two layers of fatty acid.

The temperature dependence of the conductivity shows metallic behavior for $T > 120$ K. Pauli-type behavior in the EPR spectrum down to 50 K is consistent with the assignment of metallic character. At low temperatures, $T < 120$ K, the conductivity becomes activated, and the conductivity and magnetoresistance have been interpreted within the context of a 2D electronic system with weak localization. This model is consistent with coherent carrier transport in the LB film.[79–81]

Films of this nature are not restricted to BEDO-TTF and fatty carboxylic acids.[78,82,83] Conducting films of BEDO-TTF with octadecylphosphonic acid have been produced, as have films of the donor EDT-TTF with stearic acid and octadecylsulfonic acid. The effect of UV irradiation on a BEDO-TTF stearic acid film has been studied. Extended exposure (3 h) to UV light, 14.3 mW/cm^2, caused disorder in the film that resulted in a 5-fold increase in resistance and an irreversible transformation from metallic to semiconducting behavior.[84]

3.5. LB Films Based on Phthalocyanines

Cofacial stacking of substituted phthalocyanines leads to rodlike assemblies and discotic mesophases that have attracted interest because of their highly anisotropic electronic and optical response and the prospect of solution processing. Potential applications include electroluminescent devices, electrochromic displays, organic field-effect transistors, organic light-emitting diodes, and photovoltaic cells. Phthalocyanines have long been studied in LB films.[8,10,15,85,86] Symmetric, nonamphiphilic derivatives are known to form Langmuir monolayers of face-to-face stacked macrocycles in columns parallel to the water surface.[8] The electrical properties of some examples have been studied.[15]

Recent efforts have sought to improve film processing and electronic characteristics through a series of octasubstituted phthalocyanines (**26**–**28**).[87–94] Pres-

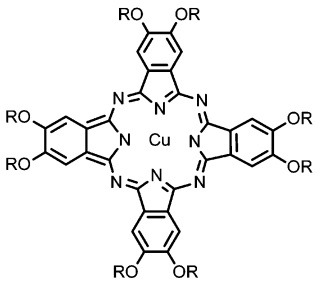

R = 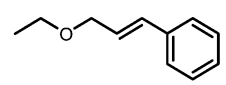 **26**

R = 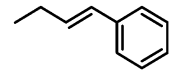 **27**

R = 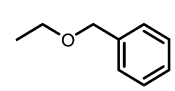 **28**

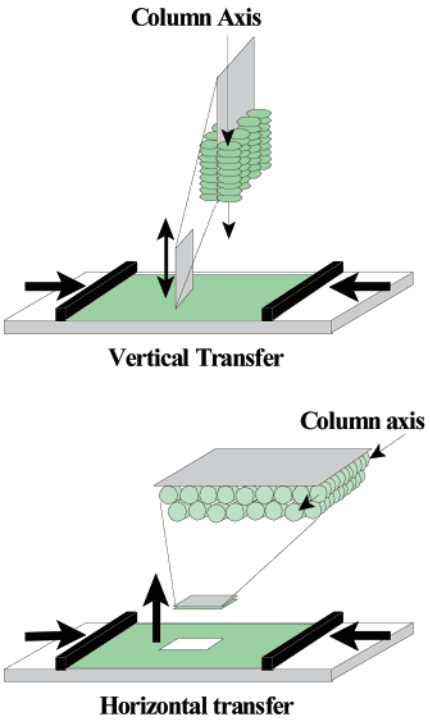

Figure 7. Schematic of the proposed molecular orientation resulting from horizontal and vertical transfer techniques of the phthalocyanine monolayers based on molecules **26**−**28** (adapted from ref 90).

sure vs area isotherms of each member of the series indicate that monolayers of the face-to-face stacked phthalocyanines form and are sustained at low pressures. Upon further compression, above 10−15 mN/m^2, the films undergo a transition, stabilizing as apparent bilayers at the air/water interface. These films can be transferred to hydrophobic supports, using either vertical or horizontal dipping methods, to yield continuous films corresponding to a bilayer thickness of columns of the stacked phthalocyanines (Figure 7). Data from a combination of AFM, X-ray reflectivity, and optical and infrared spectroscopies are consistent with the picture of aligned, partially interdigitated columns of the molecules that are often over 100 nm long. As part of the structural analysis, the authors make careful use of IR dichroism to determine the phthalocyanine orientation within the columns.[91] They explain the benefits of using both reflection−absorption infrared spectroscopy (RAIRS) and transmission FTIR spectroscopy to monitor orthogonal linear dipoles within the molecular plane to give a more accurate picture of molecular orientation.

Several important variables related to film deposition have been shown to influence the structure and properties of the transferred films. When transferred at low pressures, aggregates of the molecular columns in the monolayer assume nearly random orientation. In contrast, in the bilayer films that are deposited at higher pressure, the columns predominately align perpendicular to the barrier motion.[91] Therefore, the deposited films are highly anisotropic, with columns oriented parallel to the substrate, but also with a preferred in-plane direction. This is an important characteristic for any application that takes advantage of the anisotropic nature of the assemblies.

Annealing the deposited films at 120 °C enhances the coherence length of the columns. The surface chemistry of the substrate onto which the films are deposited also has an influence on structural coherence.[92] A phenyl-terminated surface modifier that mimics the side-chain modification of **28** improves film morphology, conformal coverage, and the resultant electrical properties.

When styryl groups are incorporated into the side chains, the solubility of the films is decreased upon postdeposition polymerization.[88] The polymerization process decreases the coherence of the columns to some extent, but the difference in solubility before and after cross-linking provides an opportunity to photopattern the deposited films.

Conductivities of the phthalocyanine films in the range 10^{-9}−10^{-8} S cm^{-1} are observed that increase 2 or 3 orders of magnitude upon electrochemical doping. Before and after doping, the conductivity along the column direction is significantly larger than the conductivity perpendicular to it, with anisotropy approaching 1000:1.[93,94] The hole mobilities of the undoped films were measured as part of preliminary investigations into the utility of the films as active materials for organic field-effect transistors. Hole mobilities about 5×10^{-4} cm^2 V^{-1} s^{-1} are observed for the unpolymerized films and increases to 1.7×10^{-3} cm^2 V^{-1} s^{-1} upon polymerization.[91,92] The authors suggest that the mobilities might actually be higher, as the measured mobilities are likely limited by the contact methods used for the measurement.

3.6. Film Structure Influence on Conductivity

The measured conductivities of LB films are consistently lower than those of related crystalline solids made up of analogous molecular building blocks. The main reason for the decreased conductivity is the granular structure of the films, with intergrain potential barriers causing thermally activated transport.[16,95,96] Macroscopic dc conductivity measurements include contributions from both intergrain barriers and intrinsic intragrain transport.

Even when quality LB films can be deposited, made up of continuous monolayers, films often contain organized domains separated by disordered domain boundaries.[95] This point was illustrated with a beautiful AFM study of a monolayer of 2-octadecylsulfanyl-*p*-benzoquinone (**29**) that clearly showed

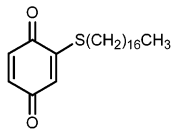

29

highly ordered domains connected by less-ordered regions.[16] Even if the domains are metallic, conductivity through the monolayer will be limited by the disordered domains. In a three-dimensional crystal, the effect of defects can be circumvented by alternative conduction pathways where structural coherence is maintained. However, in multilayered LB films,

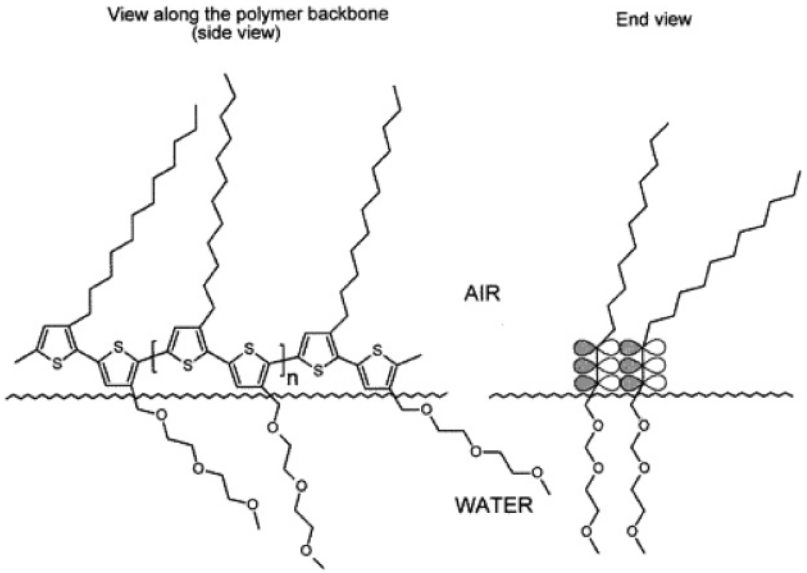

Figure 8. Single chain of regioregular amphiphilic polythiophene at the air/water interface seen from the side (left) and an end view of two adjacent π-stacking polymer chains (right) (adapted from ref 101).

the high density of aliphatic chains often separates active layers, contributing to the activation barrier.

Several recent papers have further investigated the issue of the domain structure of LB films and its effect on conductivity. Pearson and co-workers[97] demonstrated a percolation mechanism of conductivity in molecular LB films. Octadecanoyl-TTF was studied at various dilutions with octadecanoic acid. Galchenkov et al.[98] showed that surface acoustic wave (SAW) attenuation in a piezoelectric crystal resonator caused by conductivity changes in an adsorbed film provides a way to differentiate these contributions with greater sensitivity than previously explored microwave-cavity perturbation techniques. Studying LB films of a surface-active charge-transfer complex of hexadecyltetracyanoquinodimethane and heptadecyldimethyltetrathiafulvalene, $(C_{16}H_{33}\text{-}TCNQ)_{0.4}(C_{17}H_{35}DMTTF)_{0.6}$, the authors measured the temperature dependence of the conductivity using both the SAW attenuation technique and dc methods. Intragrain localization was observed and transport was evaluated using a model for quasi-one-dimensional disorder systems.

Troitsky et al.[99] further confirmed the idea that conductivity is decreased by mosaic structure. Working with C_{16}-BEDT-TTF mixed with C_{16}TCNQ, the authors used Langmuir–Schaeffer deposition methods and observed higher conductivity for thicker films, implying that mosaic domains present in thinner films are bridged across layers. Conductivities on the order of 0.52 S cm^{-1} were observed for bilayers, while thicker films had conductivities 20–60 times that. These authors also used FTIR spectroscopic and surface potential characterization of the films to highlight potential rearrangements within thin films that can lead to inhomogeneous structures.

Furthermore, contact measurements can be quite variable for thin organic films, and different electrode configurations can give different results. For example, depositing a film on top of an electrode array can give a different result than evaporating the contacts on top of the film.[100] When the electrodes are below the film, the metal will often have different contact angles than the rest of the substrate, perhaps leading to reorganization in the vicinity of the electrodes. Similarly, the film can be disrupted upon application of metal contacts on top.

Although this review has not focused on conducting polymer-based LB films, it is worth highlighting a recent example, as it illustrates the importance of some crystal engineering concepts that are also relevant to the fabrication of conducting molecule-based films. Conjugated polymers normally coil or fold. Add to this the long alkyl chains that are normally present to make the polymer amphiphilic and the interchain interactions required for high bulk conductivity are suppressed. Bjornholm and McCullough and colleagues[16,101] prepared a series of amphiphilic regioregular polythiophene derivatives with alternating hydrophobic and hydrophilic side chains. When the thiophenes in these polymers adopt the preferred transoid conformation, the hydrophilic groups are directed to allow interaction with the water, and the hydrophobic tails can then orient away from the water surface as in a traditional amphiphile. Adopting such an arrangement, these polymers form rigid board-like structures. The regular structure of the polymer chain alone is not sufficient for high conductivity in two-dimensional assemblies. The conductivity is still limited by interchain (intermolecular) interactions. The rigid board polymers facilitate these interactions as they can orient to maximize π-stacking interactions with adjacent chains (Figure 8). This assembly process on the water surface results in the formation of highly ordered crystalline domains that have been characterized with GIXD. Ordered domains are retained upon transfer to a solid support, and conductivity in I_2 or $AuCl_3$ oxidized films has been measured in excess of 100 S cm^{-1}. This value is still lower than values known for crystalline conjugated polymers, indicating that some disorder and domain boundaries

still exist. To form a conducting monolayer, intermolecular interactions in two dimensions must be optimized. This study represents an attempt to reduce the problem, fixing the interactions in one dimension with the polymer chain. Then intermolecular interactions, optimized through crystal engineering, need only be considered in one direction.

4. Magnetism in LB Films

4.1. Cooperative Magnetism in Extended Two-Dimensional Systems

4.1.1. Metal Carboxylate Films

Melvin Pomerantz and co-workers carried out the earliest extensive investigation of magnetism in LB films, working at the IBM T. J. Watson Research Center in the late 1970s.[18−20,102,103] They used careful EPR measurements to demonstrate antiferromagnetic exchange within a monolayer of manganese stearate and provided evidence for a magnetically ordered state at low temperature. Their studies had two motivations. First, one could imagine that a magnetic monolayer might be considered the ultimate magnetic memory storage device. Second, a single layer of magnetic ions provided an opportunity to investigate theoretical predictions about magnetic order in a truly two-dimensional system.

The Mn^{2+} ions were confined to a single layer between two stearate layers deposited head-to-head. The manganese stearate bilayers were formed using traditional vertical dipping onto substrates made hydrophobic with a monolayer of the nonmagnetic cadmium stearate. Evidence for magnetic exchange in two dimensions was demonstrated using EPR spectroscopy on a stacked sample of 50 slides, each containing a manganese stearate bilayer. The EPR line width and resonance field were each shown to exhibit anisotropy consistent with exchange in a two-dimensional lattice.[19,102,103] The dipolar broadening of the EPR signal depends on spin diffusion, and in 2D, it follows the form

$$\Delta H = A + B(3\cos^2 \Theta - 1)^2 \qquad (1)$$

where Θ is the angle between the external field and the film normal and A and B contain contributions from dipolar broadening. The manganese stearate data conform to this model, demonstrating antiferromagnetic exchange in a 2D array (Figure 9).

A large increase in the EPR line width below 10 K signaled a divergence of the magnetic correlation length, and a dramatic shift in the resonance field below 2 K provided evidence of an ordered state.[20,103] The anisotropy of the resonance field measured at 1.4 K is different from that seen at high temperature, signaling the development of an internal field. The authors concluded that the manganese stearate monolayers order in a canted antiferromagnetic state. The low critical temperature has made characterization of the ordered state difficult.

Other groups have studied the same system and confirmed many of Pomerantz's findings.[104] X-ray studies confirm the two-dimensional structure of monolayer and bilayer films.[105,106] Interestingly, for thicker films, the orientation of the alkyl chain differs from that of a single layer or bilayer. For multilayer films, the alkyl chain tilts approximately 30° from the normal, whereas in a monolayer, the alkyl chains are perpendicular to the substrate.[105] Haseda et al.[107] also observed magnetic ordering, although they assigned a lower ordering temperature of 0.3 K. Magnetic order in manganese stearate was also recently confirmed by a low-temperature nuclear orientation study.[106]

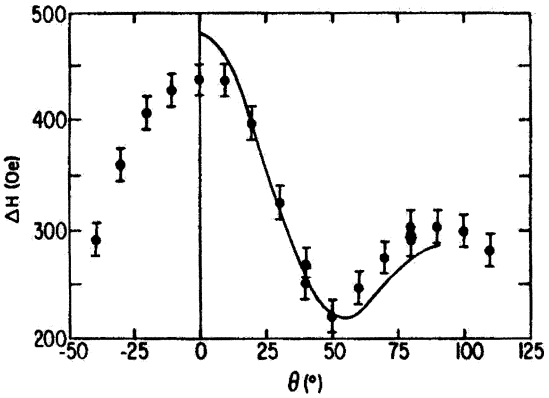

Figure 9. X-band EPR line width of an LB film of manganese stearate as a function of sample orientation. The solid line is a fit to eq 1. The behavior is consistent with dipolar magnetic exchange in a two-dimensional lattice. (Adapted from ref 102.)

It has been suggested that Langmuir−Blodgett films, as nearly free-standing magnetic layers, might be used to investigate some of the issues related to magnetic ordering in two dimensions, and this was one of the objectives of Pomerantz in his early work.[102,103] The magnetic continuous lattice is comprised of layers of exchange-coupled paramagnetic metal ions whose magnetic response is described by the spin Hamiltonian

$$\mathscr{H} = -J\sum \mathbf{S}_i\mathbf{S}_j + D\mathbf{S}_{iz}^{\ 2} \qquad (2)$$

where the exchange interaction, J, between nearest neighbors bearing spins $\mathbf{S}_i$ and $\mathbf{S}_j$ is defined by its sign, which is positive for ferromagnetic and negative for antiferromagnetic alignment of nearest-neighbor moments, and D is the single-ion anisotropy. Equation 2 says nothing about the mechanism of exchange, but in most LB films, a superexchange mechanism operates, whereby magnetic interactions within a layer are modulated by an active ligand that bridges adjacent metal ions. Dipolar interactions, which are normally small but can be active over very large distances, are also possible.[108]

Two-dimensional systems have been of great interest since Bloch,[109] later supported by the Mermin−Wagner theorem,[110] argued that an isotropic interaction in a one- or two-dimensional lattice will not lead to long-range order at a finite temperature. This result is often quoted, but in practice, an ideal isotropic two-dimensional system is difficult to realize, and most synthetic 2D model systems order.[103] Magnetic ordering can result if there is any anisotropy in the system, such as nonequivalent spin

components ($\mathbf{S}_{ix} \neq \mathbf{S}_{iy} \neq \mathbf{S}_{iz}$) or single-ion anisotropy ($D \neq 0$), or if there is a small contribution, such as dipolar interactions, to interlayer magnetic exchange ($J_\perp \neq 0$). A number of theoretical papers address magnetic interactions in LB films and related systems.[111–115]

Although ordering has been seen in manganese stearate by Pomerantz and others, these monolayer films might not be perfect models for probing the Mermin–Wagner theorem, as long-range dipole–dipole interactions might violate the assumptions leading to the theorem. Long-range order has now been observed in several different Langmuir–Blodgett film systems, and it has thus far proven difficult to identify the specific interactions responsible for the magnetic ordering.

Similarly, the magnetic properties of fatty acid salts of other divalent metals have also been studied.[116,117] Ando et al.[117] looked at stearate films of Mn^{2+}, Fe^{2+}, Co^{2+}, and Ni^{2+}. Under normal deposition conditions, Fe^{2+} is difficult to handle, and the authors indicate that the iron films might not be a single phase, but rather a mixture of oxidation states or spin states.[116] Structural and EPR studies of the manganese stearate film confirm earlier results. The SQUID data on the Mn^{2+}, Fe^{2+}, and Co^{2+} films show negative Weiss constants and are presented as evidence for antiferromagnetic exchange. The Ni^{2+} film gave a Weiss constant of 2 K, and the authors suggest ferromagnetic interactions, although single-ion effects were not considered.

Iron(III) arachidate films have also been studied,[118–120] and Mössbauer spectroscopy indicates antiferromagnetic ordering below 130 K. Highly sensitive conversion electron Mössbauer spectroscopy (CEMS) was performed down to 90 K, and absorption Mössbauer experiments were performed to 4.2 K and in the presence of a magnetic field. The appearance of an antiferromagnetically split sextet below 130 K indicates antiferromagnetic order. Analysis shows that 86% of the film is in the ordered state, with 14% remaining paramagnetic. Multilayered LB films were chemically characterized by mass spectrometry, which showed that arachidate was completely in the salt form. EPR spectroscopy and Mössbauer measurememts were consistent with Fe^{3+}, and X-ray diffraction confirmed the layered structure of a multilayered assembly. The chemical analysis of the film appears sound, although characterization of the topography of the film was not presented.

LB films of gadolinium stearate[121–125] have been reported to show evidence of a magnetically ordered state with a transition temperature near 500 K. Changes in the EPR line width and resonance field are cited as evidence of ordering.[121,124] It is unlikely, though, that the as-deposited film retains its structure upon excursions to these temperatures. Surface inhomogeneites, seen even at room temperature,[123] might be responsible for some of the reported observations. The same system, prepared and studied by Mukhopadhyay et al.,[126] reveals no magnetic ordering down to 2 K in the absence of applied field, although field-induced ferromagnetism at low temperatures is observed in the in-plane direction.

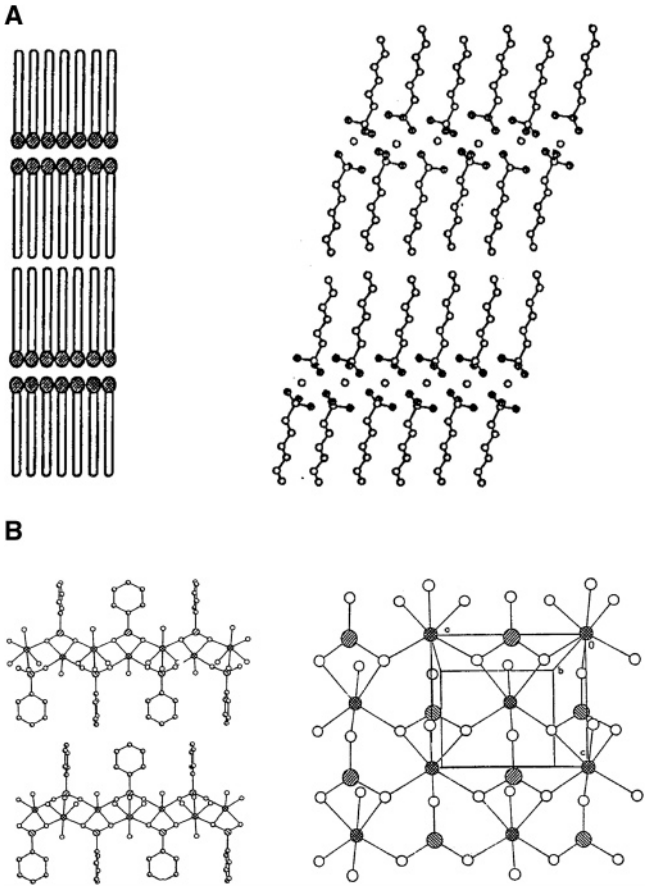

Figure 10. (a) Scheme illustrating the similar layered structures of a Y-type LB film (left) and the layered metal alkylphosphonate exemplified by $Ca(O_3PC_6H_{12})_2$ (right). (b) Layered nature of $Mn(O_3PC_6H_5)\cdot H_2O$ shown in a cross section (left) and manganese ion plane viewed perpendicular to the layer (right), where the phenyl groups have been omitted for clarity. (Adapted from ref 128.)

4.1.2. Metal Phosphonate LB Films

Related to the metal arachidate and stearate LB films are the metal salts of alkylphosphonic acids (Figure 10). For example, octadecylphosphonic acid, **30**, forms LB films with a variety of divalent, trivalent, or tetravalent metal ions resulting in layers of the metal ions sandwiched within bilayers of the organophosphonate.[127–131] What is significantly different from the metal carboxylate films is that solid-state metal phosphonates form layered continuous lattice structures, so that it has been possible to learn details about the in-plane structure of the LB films by comparing them to the known solids.

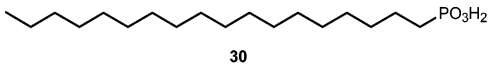

30

The most extensive magnetic studies have been on manganese phosphonate LB films.[128,132–137] In the solid state, manganese alkylphosphonates crystallize in the orthorhombic space group $Pmn2_1$.[138] Sheets of manganese ions, in a distorted square array, are bonded on top and bottom by layers of the organophosphonate (Figure 10b). Within a layer, each phosphonate group bridges four metal ions, and each metal ion is coordinated by five oxygen atoms from four different phosphonate groups. The distorted

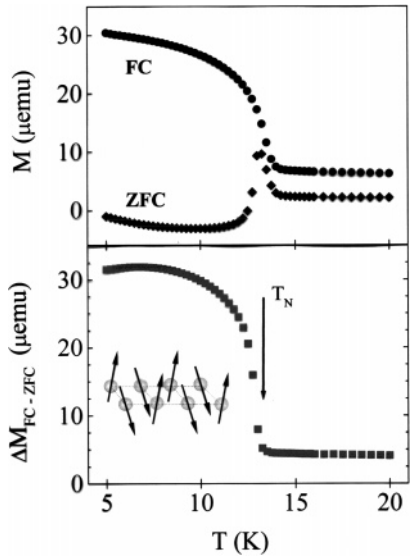

Figure 11. Magnetic ordering to a canted antiferromagnetic state is observed at 13.5 K in an LB film of manganese octadecylphosphonate. (Top) Field-cooled (FC) and zero-field-cooled (ZFC) magnetization plots. (Bottom) Difference between the FC and ZFC magnetizations (ΔM). Because the mass of the sample is small compared to the sample holder and Mylar substrate, the difference plot subtracts the signal due to the sample support and allows the film magnetization to be quantified. (Adapted from ref 128.)

octahedral coordination of the metal is completed by a water molecule. Magnetic exchange within the layers is antiferromagnetic, and the solid-state alkylphosphonates $(C_nH_{2n+1}PO_3)Mn\cdot H_2O$ ($n = 2-6$) each order antiferromagnetically between 13 and 15 K.[139,140] A weak moment develops below the ordering temperature, and the solid-state phosphonates are known to be canted antiferromagnets.[128,137,139,140]

Manganese octadecylphosphonate LB films have been shown to have the same in-plane structure as the related solid-state compounds.[128,141] At high temperatures, the EPR behavior is reminiscent of manganese stearate LB films, consistent with antiferromagnetic exchange within the 2D sheets.[136] The temperature dependence of the EPR intensity was used to estimate the magnitude of the nearest-neighbor exchange, J, by fitting the data to a numerical expression for the susceptibility of a quadratic layer Heisenberg antiferromagnet. The value of $J/k_B = -2.8$ K obtained from the fit is nearly identical to the values of exchange constants observed for the solid-state manganese phosphonates. A magnetic ordering transition is observed in static magnetization measurements (Figure 11).[128] The LB film also exhibits magnetic memory below T_N. Hysteresis is observed in the vicinity of zero field for positive and negative scans of the applied field as it is cycled between ± 5 T.

4.1.3. Metal Cyanide Networks

Metal cyanide extended networks, two-dimensional analogues of Prussian Blue, have also been fabricated as part of Langmuir−Blodgett films. Metal cyanides have been of interest to the molecule-based magnetism community[142−145] because the nature of the magnetic exchange can be anticipated in advance from basic orbital interaction arguments and the predictable structure-directing quality of the cyanide bridge.[146] This inherent ability to tailor both the structure and magnetic exchange in metal cyanide systems makes this family of materials well-suited for studying molecule-based magnetic phenomena. A wide range of magnetic phenomena have been observed in metal cyanides, including high-spin clusters,[147−152] metamagnetism,[146,153−155] room-temperature magnetic ordering,[156−158] spin-glass behavior,[159,160] and photomagnetism.[161−163] These cubic inorganic solids have the general formula $A_k[B(CN)_6]\cdot nH_2O$, where A and B can be divalent or trivalent transition metals and k depends on the relative charges of the different metal ions and the number of vacancies in the structure. Charge-balancing monovalent cations might also be present.

LB films of Prussian Blue related compounds were first prepared by Mingotaud and co-workers[164,165] by spreading a positively charged lipid such as dioctadecyldimethylammonium ion (DODA) on a very dilute colloidal dispersion of "soluble" Prussian Blue, $Fe_4[Fe(CN)_6]_3\cdot 12H_2O$,[164,165] or the mixed-metal analogue $Cu_3[Fe(CN)_6]_2\cdot 12H_2O$.[166] The monolayers can be transferred to form Y-type films with the inorganic metal cyanide species trapped within the amphiphilic bilayer. The exact state of the metal cyanide species is quite sensitive to the deposition conditions.[167] Higher subphase concentrations lead to "rough" films, indicating that colloidal particles are transferred. However, at very low concentrations, molecular species that are present in the subphase as a result of the dissociation of the colloidal particles appear to reassemble into a lamellar network.[167]

A ferromagnetic ground state is observed for both the Fe^{2+}/Fe^{3+} and the Cu^{2+}/Fe^{3+} mixed-metal films. The Curie temperature for the Fe^{2+}/Fe^{3+} film is assigned as $T_C = 5.7 \pm 0.1$ K, which is slightly higher than the value determined under the same experimental conditions for the commercial Prussian Blue powder used as the precursor ($T_C = 5.1 \pm 0.1$ K).[23,165] The higher ordering temperature might be due to changes in structure, or it could be a result of the anisotropic nature of the thin film. Strong anisotropy in the EPR line position (g factor) and the line width (ΔH in gauss) near T_C are consistent with a two-dimensional magnetic system. A similar result is observed for the mixed-metal system.[166] The pristine powder sample orders at $T_C = 21$ K, whereas the corresponding LB film has $T_C = 25$ K. Both the Fe^{2+}/Fe^{3+} and the Cu^{2+}/Fe^{3+} films show hysteresis in plots of magnetization vs applied field below T_C, characteristic of the presence of magnetic domains inside a soft ferromagnetic state (see Figure 12).

A different approach for preparing a metal cyanide network within an LB film is to include one of the metal sites in an amphiphilic complex. Reaction of a Langmuir monolayer of the amphiphilic pentacyanoferrate(III), **31**, with Ni^{2+}, Co^{2+}, or Mn^{2+} ions from the subphase results in two-dimensional mixed-metal cyanide-bridged networks at the air/water interface (Figure 13).[168−170] Confinement of the reactants to the air/water interface discriminates against the forma-

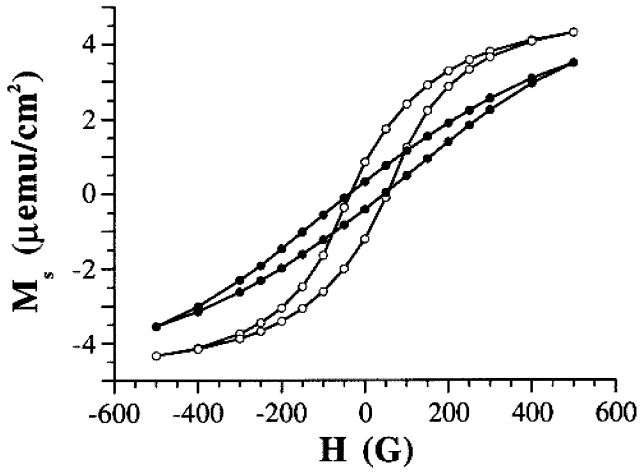

Figure 12. Hysteresis loops of a 300-layer Prussian Blue/DODA LB film at 2 K with the magnetic field parallel (○) and perpendicular (●) to the LB layers (adapted from ref 165).

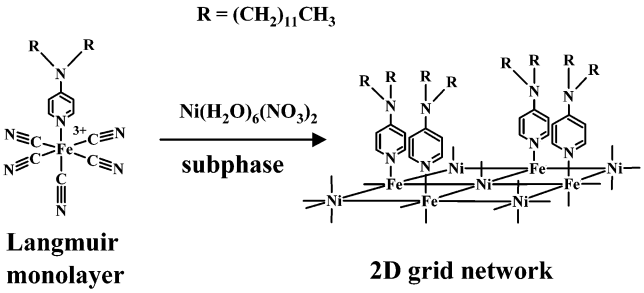

Figure 13. Reaction of an amphiphilic pentacyanoferrate complex, **31**, confined to the air/water interface with aqueous Ni^{2+} ions results in a mixed-metal cyanide bridged square-grid network (adapted from ref 168).

tion of higher-dimensionality products and directs the lateral propagation of the two-dimensional network.

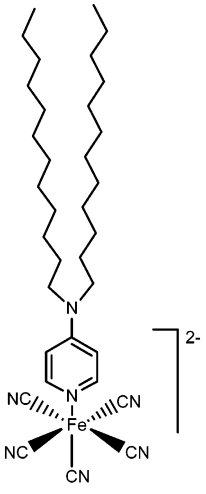

31

The networks can be transferred to various supports to form monolayer or multilayer lamellar films. The structure of the networks was confirmed with grazing incidence synchrotron X-ray diffraction (GIXD), which revealed a face-centered square-grid structure for each example with cell edges in the range of 10.2−10.4 Å, as expected on the basis of the related two- and three-dimensional solid-state analogues. X-ray photoelectron spectroscopy (XPS), FTIR spectroscopy, and X-ray absorption fine structure (XAFS) spectroscopy confirm the chemical structure of the film. The same network does not form from homogeneous reaction conditions. Therefore, the results demonstrate the potential utility of an interface as a structure director in the assembly of low-dimensional coordinate covalent network solids.

Magnetic susceptibility measurements on multilayered samples indicate that the Fe−Ni network undergoes a transition to a ferromagnetic state below $T_C = 5.4$ K.[168,170,171] A frequency dependence in both the real and imaginary components of the ac susceptibility is interpreted as being characteristic of spin-glass-type ordering of the ferromagnetic domains to form a cluster glass. Domains are likely limited by structural coherence, shown by GIXD to be approximately 60−80 Å. The ferromagnetic behavior of this system is rationalized by realizing that, for octahedral metal centers, the magnetic orbitals are the Fe^{3+} ($S = {}^1/_2$) t_{2g} and the Ni^{2+} ($S = 1$) e_g sets, and that the cyanide orbitals that overlap with them are orthogonal. For the Fe^{3+}/Ni^{2+} LB film, the ordering temperature is lower than the $T_C = 23$ K observed in the cubic analogue, but it is similar to the ordering temperature reported in other low-dimensional Fe−CN−Ni networks.[153] Networks formed from **31** with Mn^{2+} of Co^{2+} are also magnetic at low temperature.[169]

Single-layer control over the deposition process provides an opportunity to observe how the magnetic properties of the system evolve as it changes from a monolayer to a bilayer to a multilayer film. The Fe−Ni two-dimensional (2D) network was transferred as an isolated monolayer, as a single bilayer, or as multiple-bilayer assemblies (Figure 14),[170] and the magnetic response of these films in the range 2 K < T < 300 K in dc fields of 2 kG < H < 50 kG and in 4 G ac fields from 1 Hz to 1 kHz were studied. A lower glass temperature (T_g) is observed in the isolated monolayer film that increases in the bilayer and further increases in the multilayer film. Similarly, the magnetic coercivity increases from monolayer to bilayer to multilayer (Figure 15). The different magnetic responses of the three films are attributed to different in-plane, interplane, and long-range dipolar exchange interactions. This series shows that long-range magnetic dipolar interactions across distances greater than 30 Å can be important in such assemblies.[172]

4.2. Cooperative Magnetism in Purely Organic Molecular Systems

There have been many studies of magnetic measurements on organic LB films. In particular, there have been numerous examples of EPR analyses of radicals in LB films for the purpose of understanding film structure, molecular orientation, or molecular dynamics.[173] Many of the LB films of organic radicals discussed in the first part of the present article have been probed using EPR spectroscopy. However, we limit our discussions here to systems for which magnetic properties were the objective behind the studies. There are relatively few examples, and all center on amphiphilic nitronyl nitroxide radicals.

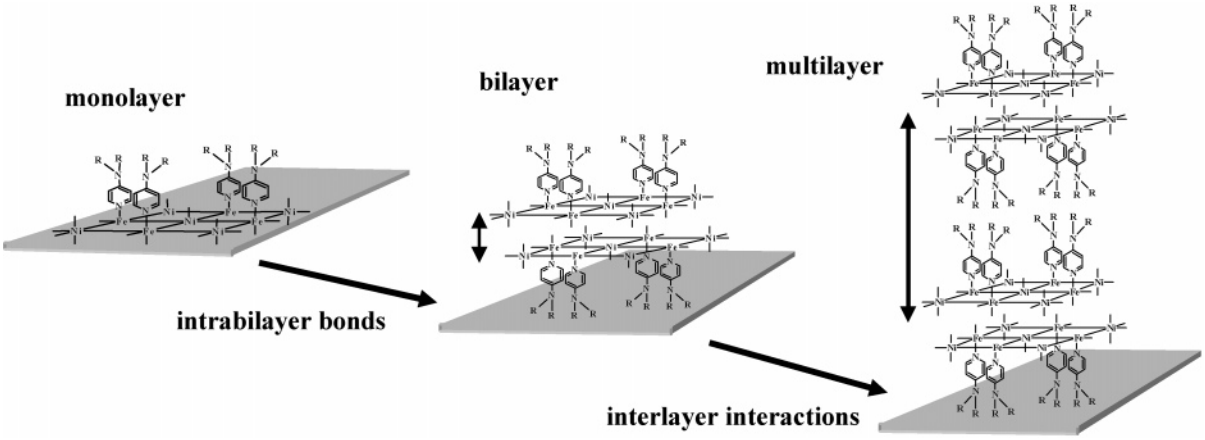

Figure 14. Two-dimensional cyanide-bridged $Fe^{III}-Ni^{II}$ square-grid networks assembled at the air/water interface and subsequently transferred using the Langmuir−Blodgett technique as monolayer, bilayer, and multiple bilayer (multilayer) films results in novel low-dimensional systems in which the effects of dimensionality on magnetic behavior in molecule-based materials can be observed (see Figure 15). (Adapted from ref 170.)

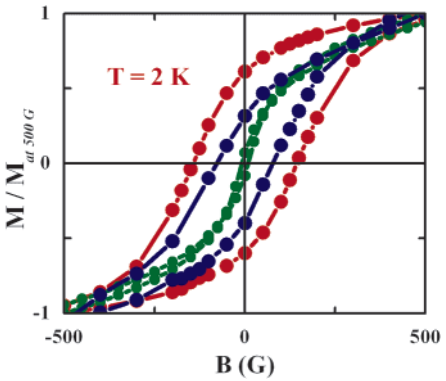

Figure 15. Magnetization vs applied field plots showing the increasing hysteresis when comparing a monolayer, bilayer, and multilayer of the cyanometalate structures depicted in Figure 14. Different magnetic responses of the three films are attributed to differences in the in-plane, interplane, and long-range dipolar exchange interactions.

The radical **32** was synthesized by Le Moigne et al.[174] and characterized in an LB film. Magnetic

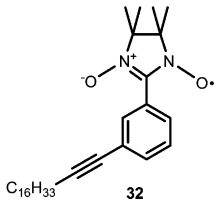

32

data[175] for an LB monolayer were compared to those for the same molecule in a cast film. The SQUID magnetometry reveals weak antiferromagnetic interactions in the cast film, with a Weiss constant of $\theta = -0.9$ K. In contrast, a monolayer deposited onto silica displays ferromagnetic interactions in EPR measurements. The EPR line shape is Lorentzian in the LB monolayer, differing from that of the cast film. Analysis of the line shape and anisotropy of the g value and line width are consistent with exchange in a two-dimensional network. The temperature dependence of the magnetic susceptibility, derived from the EPR intensity, yields a positive Weiss constant, $\theta = 2.5$ K, indicating ferromagnetic interactions. The result shows that the Langmuir−Blodgett technique provides some degree of control over intermolecular magnetic interactions. The molecular organization in the monolayer, where the headgroup interacts with the silica substrate, provides for different exchange pathways than are present in the cast film.

Bai and Zhu and co-workers[176,177] prepared the amphiphilic radical **33** and studied films at room temperature with EPR spectroscopy and magnetic force microscopy. To increase intermolecular spin−spin interactions, the diradical **34** was prepared.[178] The temperature-dependent susceptibility, also determined from EPR intensity, reveals strong antiferromagnetic interactions.

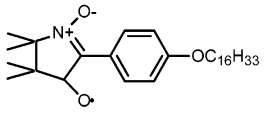

33

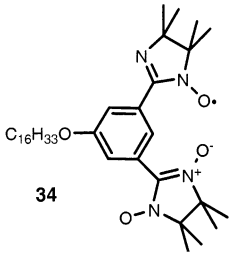

34

4.3. Magnetic Effects Derived from Molecular Properties in LB Films

A series of polyoxometalate ions have been included in LB films by incorporating them as counterions to cationic surfactants such as DODA or DPPC (Figure 16).[179−181] Polyoxometalates are inorganic clusters with the general formula $X_aM_bO_c^{n-}$ (M = Mo, W, V, and X = P, Si, B, Co). The best known of these are the Keggin ions that are based on a central heteroatom surrounded by four M_3O_{13} groups (M = Mo, W). Spectroscopic analysis of an LB film with X = Co, M = W, $(CoW_{12}O_{40})^{6-}$, indicates that the heteropolyanion is included between DODA layers and that the Keggin polyanions are not randomly oriented within the film, but rather adopt one particular orientation or structural distortion. Magnetic measurements exhibit a decrease in susceptibility at low temperature that originates from the zero-field splitting of Co^{II} in a tetrahedral environment.[179]

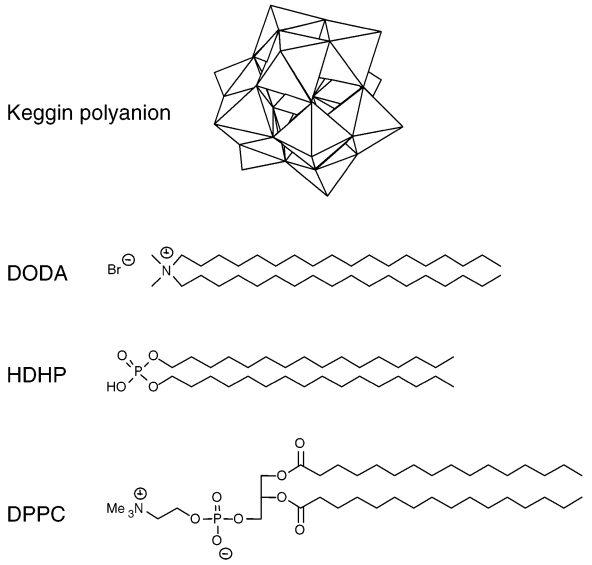

Figure 16. Molecular structure of a Keggin polyanion and amphiphiles used to include it in LB films (adapted from ref 181).

Other polyoxometalate clusters have been incorporated into LB films as well. A tungsten atom in the periphery of the Keggin ion can be exchanged by a Mn^{II} ($S = {}^5/_2$) ion to add paramagnetism. The ion $[SiMn(H_2O)W_{11}O_{39}]^{6-}$ was transferred with DODA, as was the cluster $[Co_4(H_2O)_2(PW_9O_{34})_2]^{10-}$.[180] Largely, the magnetism of the LB assemblies indicates that the clusters are magnetically isolated. For the tetrameric cobalt cluster, ferromagnetic exchange interactions occur within the cluster leading to a total spin of $S = 6$, and the magnetic properties of the corresponding LB film reflect this, deviating from the Curie law and thereby indicating intramolecular ferromagnetic interactions. A decrease of the product χT at very low temperature suggests the presence of a magnetic ground state with a smaller spin multiplicity.[180]

In the solid state, a series of mixed-metal transition metal oxalates form lamellar extended systems with a range of magnetic properties.[182–184] Related to these extended systems, the monomeric metal oxalate complexes $[Fe(C_2O_4)_3]^{3-}$ and $[Cr(C_2O_4)_3]^{3-}$ can be associated with charged surfactants such as DODA and transferred as LB films.[185] It was shown that the metal oxalate complexes are organized within the LB film as monolayers trapped between organic bilayers. The complexes are noninteracting, and the magnetic behavior of the films is simply described by the Curie law. A series of heterobimetallic complexes such as the $Cr^{III}–Fe^{II}–Cr^{III}$ polyoxalate $[Fe(H_2O)_2(Cr(C_2O_4)_3)_2]^{4-}$ were similarly deposited between DODA layers. These complexes also behaved as isolated ions, although deviation from the Curie law at low temperature indicates weak intramolecular magnetic interactions.[185]

4.3.1. Single-Molecule Nanomagnets

Arrays of single-molecule magnets have been constructed using Langmuir–Blodgett methods.[186–188] High-spin magnetic clusters with large magnetic hysteresis provide the possibility of molecular bistability and information storage at the molecular level.[189] The most thoroughly studied single-molecule magnets are the mixed-valence manganese clusters based on the Mn_{12} core of the prototype $Mn_{12}O_{12}(O_2CCH_3)_{16}(H_2O)_4$. They are formed by an internal tetrahedron of four Mn^{IV} ions ($S = {}^3/_2$) surrounded by eight Mn^{III} ($S = 2$) ions. Exchange interactions within the cluster result in a ground state with a large spin, $S = 10$, that encounters a thermal barrier for reversal of the direction of magnetization along the uniaxial magnetic axis ($D \neq 0$, see eq 2). In the crystalline state, these neutral clusters exhibit a stable hysteresis loop with a coercive field as large as 1.5 T at 2 K.[189] In addition, these nanomagnets provide unique examples for observing quantum magnetization effects. Attempts to use single-molecule magnets for information storage will require methods to organize them into arrays on surfaces.

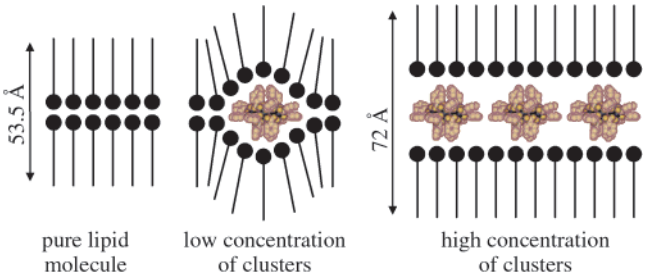

Figure 17. Schemes of the Y-type Langmuir–Blodgett films formed from Mn_{12} single-molecule magnet clusters as the lipid/cluster ratio is varied (adapted with permission from ref 188).

Initial experiments were performed with $Mn_{12}O_{12}(O_2CCH_3)_{16}(H_2O)_4$ and the corresponding benzoate derivative, $Mn_{12}O_{12}(O_2CC_6H_5)_{16}(H_2O)_4$. By themselves, the clusters do not form stable Langmuir monolayers, so films are prepared by mixing them within a matrix of behenic acid.[186,188] The degree of organization of the Mn_{12} clusters within the LB film depends strongly on the lipid-to-cluster ratio, as illustrated in Figure 17. For ratios near 5:1, a lamellar structure forms with two-dimensinoal arrays of clusters. At lower ratios, the clusters become isolated, and the lamellar structure is disturbed. Films containing the Mn_{12} clusters show hysteresis in the magnetization vs applied magnetic field (**M** vs **H**) response at 2 K. The coercive field for the film containing the acetate cluster is 0.06 T, whereas that for the benzoate is 0.1 T. The response is anisotropic, with a softer hysteresis loop when **H** is parallel to the plane of the magnetic monolayer than when **H** is perpendicular, reflecting the anisotropic nature of the cluster array within the film. The magnetic properties of the clusters in the film differ substantially from those of crystalline samples of the single-molecule magnets. The coercivity is much reduced in the films, and the magnetization at 5 T is significantly less than saturation.[186,188]

Exchange of the acetate or benzoate ions for stearate gives the cluster $Mn_{12}O_{12}(O_2C(CH_2)_{16}CH_3)_{16}(H_2O)_4$. It was hoped that the presence of the longer aliphatic groups would aid in spreading of the cluster without the need for cosurfactant.[187] Unfortunately, multilayers spontaneously form on water, and mono-

layer films were not generated. Mixing the stearate cluster with a cosurfactant does result in a monolayer. The magnetic behavior of the transferred film resembled the that of LB films of the acetate and benzoate analogues.[187]

Monolayers of a related cluster, $Cr_8O_4(O_2CPh)_{16}$, at the air/water interface have been structurally characterized with GIXD and X-ray reflectivity.[190] These studies show that monolayers form at low surface pressures, 3−5 mN/m, in contrast to the $Mn_{12}O_{12}(O_2CPh)_{16}$ case just described, although structural correlation lengths are small, extending over a few molecular distances. At higher pressures, the film becomes less compressible, but a second layer begins to form on the first. The $Cr_8O_4(O_2CPh)_{16}$ cluster was not studied in transferred films.

4.3.2. Spin-Crossover Compounds

Spin-crossover or high-spin/low-spin transitions have long been of interest in studies of molecular magnetism.[191] The spin-state transition corresponds to a change in magnetic susceptibility but is accompanied by structural and spectroscopic changes as well. For example, in some cases, the spin transition is signaled by dramatic changes in color. This marriage of optical and magnetic properties has made spin-crossover compounds the subject of study as potential read-write information storage media.[192]

Thermally induced spin crossover can occur gradually, reflecting the thermal populations of the two close-in-energy spin states. Alternatively, the transition can be abrupt, sometimes occurring within a few kelvin. Because spin transitions involve changes in metal−ligand bonding, the occurrence of a smooth or abrupt transition is related to the coupling of the compound's electronic structure to the environment, or crystal lattice. Smooth transitions occur in solution or when interactions with the lattice are small. On the other hand, if the lattice is too rigid, spin-crossover transitions can be suppressed completely. Abrupt transitions reflect strong coupling to a lattice that can support the requisite changes in structure that accompany a spin transition, but in a cooperative event. In such cases, there is the possibility of hysteresis in the temperature dependence of the spin state and, therefore, the bistability desired for information storage.[191,192]

Spin crossover in Langmuir−Blodgett films has been studied in an effort to influence the electronic spin-state interconversion of complexes by purposefully controlling their condensed-phase environment. The first attempts were made by Ruaudel-Texier et al.,[193] who prepared an amphiphilic bis-phenanthroline-bis-thiocyanato iron(II) complex based on ligand **35**. Changes in C−N stretching frequencies between

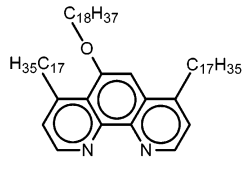

35

room temperature and 77 K indicated spin crossover

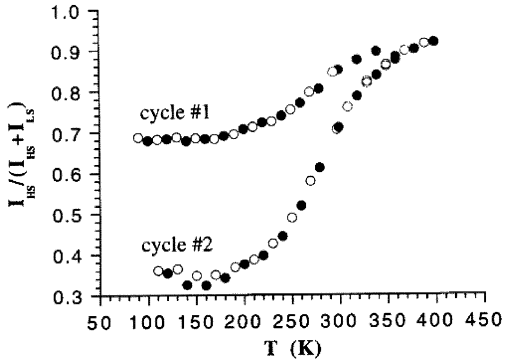

Figure 18. High-spin to low-spin transition in an LB film of **36** evidenced by IR spectroscopy. The ratio $I_{HS}/(I_{HS} + I_{LS})$ is determined from the integrals of the IR peaks between 2090 and 2135 cm^{-1} (noted I_{LS}) and between 2000 and 2090 cm^{-1} (noted I_{HS}). Key: (○) decreasing temperature, (●) increasing temperature. First thermal cycle: 300 → 100 → 400 K. Second thermal cycle: 400 → 100 → 400 K. (Adapted from ref 196.)

in an LB film of the complex. However, the complex is unstable to the LB processing conditions, so quantitative measurements were not possible. Similarly, attempts were made to form an LB film of an iron(II) coordination polymer of the ligand octadecyl-1,2,4-triazole that shows a spin transition in the bulk, but the polymeric complex is also unstable on the air/water interface.[194]

More recently, amphiphilic complexes **36** and **37**, modeled after the parent iron(II) bipyridine complex Fe^{II}(4,4′-dimethyl-2,2′-bipyridine)$_2$(NCS)$_2$ with a transition temperature near 270 K, have been prepared.[195−197] Two strategies were developed to overcome problems with the chemical and physical stability of these complexes in Langmuir monolayers. The first, in the case of complex **36**, was to transfer the Langmuir monolayer from a mixed subphase containing formamide instead of pure water in order to decrease hydrolysis of the complex.[196] A second approach to reducing hydrolysis was to modify the chemical structure of the bipyridine ligand and avoid the need to work with organic solvents. Complex **37**,

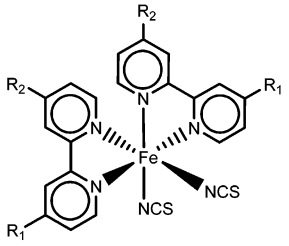

R_1 = -$C_{17}H_{35}$
R_2 = -CH=CHPh **36**

R_1 = -$(CH_2)_{12}$-$(CF_2)_5$-CF_3
R_2 = -CH_3 **37**

with semi-fluorinated chains, shows a remarkably enhanced stability on a 10^{-2} M KNCS aqueous solution.[195]

The spin states of the complexes were followed by monitoring the magnetism, as well as by monitoring the C−N stretch of the NCS^- ligands. Compound **36** shows a thermal history dependence (Figure 18).[196,197] During the first thermal cycle, the spin-crossover process is partially reversible and centered around 292 K, as in the pristine powder. However, in contrast to the bulk, the transition is not complete. A large quantity of the iron complex is trapped in

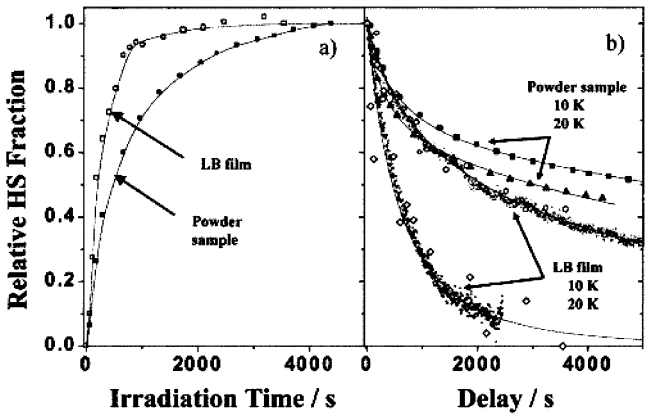

Figure 19. (a) Relative HS molar fraction of compound **37** deduced from magnetic measurements under light irradiation as a function of time at 10 K. (b) Decay of the metastable HS state. (Adapted from ref 198.)

the low-spin state upon film transfer and does not undergo the spin-conversion process within the LB film. These results suggest that the LB film-forming process influences the environment of the metal complexes and might be used to control the spin-transition event. Similar behavior was observed for compound **37**.[195]

If the multilayer is heated above 330 K, then most of the film undergoes the spin transition in a second thermal cycle (Figure 18).[196] Such behavior agrees with the hypothesis that the LB packing influences the molecular environment. Heating the LB films above 330 K allows the alkyl chains to disorder, leading to relaxation of the structure previously induced by the LB deposition process.

Photoinduced spin crossover, or the LIESST effect (light-induced excited spin-state trapping), has been observed for an LB film of **37**.[198] Irradiating the LB film at 10 K, using wavelengths corresponding to the MLCT of the low-spin state, results in spin transition to the high-spin state (Figure 19). Relaxation of the LIESST state of the LB film of **37** was compared to the behavior of a bulk sample. Different relaxation dynamics provide further evidence that the LB environment is not the same as the bulk environment, providing a way to control these spin-transition effects.

5. Hybrid Films and Dual-Network Assemblies: Attempts to Mix Properties

The very nature of Langmuir–Blodgett films makes them ideal platforms for combining more than one targeted property into a single material. The layer-by-layer deposition process and the amphiphilic nature of the basis molecules both provide avenues for introducing multiple functions into one film. By changing the basis molecules from one layer to the next, superstructures can be built in which the chemically different layers contribute different physical properties. Alternatively, the segregated hydrophobic and hydrophilic character of LB films can lead to mixed organic/inorganic films, or dual-network assemblies, where the organic and inorganic components contribute separate properties (Figure 1).[23,199] In either case, the partnered components can either work independently, providing a material with composite properties, or work in synergy, potentially producing new phenomena. Examples involving conducting or magnetic LB films usually involve introduction of a photoactive or electroactive component designed to switch the property of interest with external stimulus. In addition, films that are both conducting and magnetic have also been targeted.

The photochemical switching of LB film conductance was attempted in two recent studies, already described above. Semiconducting films were formed from the azobenzene-derivitized TTF **21** after iodine doping.[56] However, the trans-to-cis isomerization of the azobenzene groups normally seen upon UV illumination was not observed, presumably because the packing of the chromophores was too tight, and no change in conductivity was observed. A related example in a TCNQ-based film did exhibit conductivity changes upon irradiation. A complicated multilayer assembly including the $[TCNQ_2]^-$ salt of the pyridinium amphiphile **9** mixed with a cyanine dye amphiphile forms semiconducting films.[41] Alernate irradiation with UV light and visible light increases and decreases conductivity, although the process quickly degrades the film's conductance.

Photochemical switching of magnetic properties with azobenzene chromophores has also been attempted. Manganese phosphonate LB films of the chromophore **38** have been prepared.[200] Spectroscopic

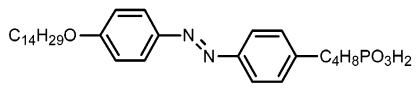

38

analysis and GIXD confirm that the same extended lattice inorganic network observed for the octadecylphosphonate LB films forms even in the presence of the azobenzene group.[141,200] The film also orders magnetically, becoming a canted antiferromagnet below 14 K, providing further evidence that the inorganic network forms (Figure 20). Unfortunately, trans-to-cis isomerization of the azobenzene is not effected upon UV irradiation. The close packing of the azobenzene chromophores in the mixed organic/inorganic film does not provide the flexibility and free volume needed for the isomerization to occur. As a result, there is no change in magnetic response with illumination.

A hybrid film containing Prussian Blue and an electroactive and photoactive tris-bipyridyl ruthenium(II) amphiphile, **39**, has been developed,[167,201]

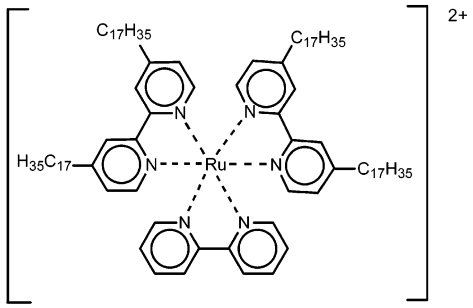

39

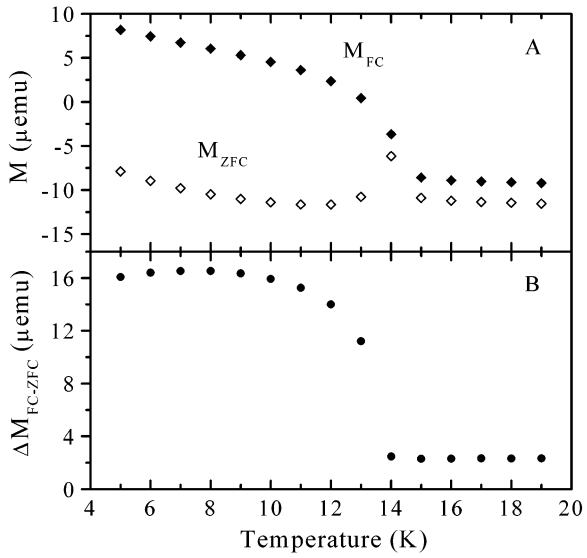

Figure 20. Magnetization vs temperature for a 100-bilayer sample of the manganese phosphonate film based on compound **38**. (A) Field-cooled (M_{FC}, 0.1 T) and zero-field-cooled (M_{ZFC}) data with a measuring field of 0.01 T. (B) difference between the FC and ZFC data showing a net magnetization below T_N, 14 K, which is evidence for spontaneous magnetization to a canted antiferromagnetic state. (Adapted from ref 200.)

similar to the Prussian Blue/DODA system described previously. This example with the ruthenium complex is also magnetic and helped elucidate the mechanism of Prussian Blue inclusion in these films. Prussian Blue is also electroactive and photoactive, and the chromophores were shown to act together to produce a large cathodic photocurrent when the hybrid film was illuminated.[201] However, any influence of the ruthenium complexes' optical properties on the magnetism in the Prussian Blue network has not yet been reported.

A hybrid film formed by alternating layers of magnetic polyoxometalate clusters and an organic donor molecule has been reported by Clemente-Leòn et al.[202] The cluster $[Co_4(H_2O)_2(P_2W_{15}O_{56})_2]^{16-}$ was transferred with a monolayer of the cationic surfactant DODA, as described in an earlier work and discussed above. A monolayer of the semi-fluorinated donor, **40**, was then transferred onto the hydrophobic

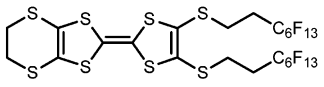

40

surface provided by the DODA layer. Repeating the process of alternately depositing layers of DODA/POM and **40** results in the hybrid film shown schematically in Figure 21. X-ray diffraction of the deposited film indicates a periodicity that is consistent with a layered superstructure in the figure. Iodine vapor treatment oxidizes the donor, leading to an electronic absorption in the IR region consistent with charge delocalization. However, the macroscopic conductivity did not increase after oxidation, suggesting that the structure of the film did not permit long-range delocalization.

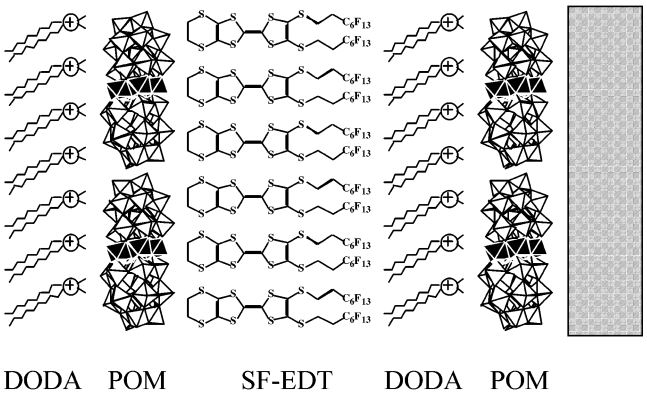

Figure 21. Proposed structure of a hybrid organic/inorganic LB film. SF-EDT is compound **40**. POM is the polyoxometalate cluster $[Co_4(H_2O)_2(P_2W_{15}O_{56})_2]^{16-}$. (Adapted with permission from ref 202.)

Petruska et al. prepared a mixed organic/inorganic dual-network LB film in which the polar network is the magnetic manganese phosphonate lattice and the organic network contains the bis(phosphonic acid) amphiphile 2,3-bis(4′-phosphonic acid-butylthio)-6,7-bis(tetradecylthio)tetrathiafulvalene, **41**.[134,135] LB depo-

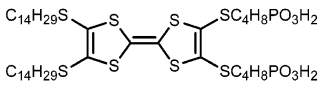

41

sition of **41** from an aqueous Mn^{2+} subphase forms Y-type films with stoichiometry $Mn_2(\mathbf{41})(H_2O)_2$. Because the donor has two alkylphosphonate arms, the film stoichiometry is consistent with the $Mn(O_3PR)\text{-}H_2O$ structure known in other manganese phosphonate LB films and layered solids. The film becomes magnetic near 11.5 K when the manganese phosphonate network orders as a canted antiferromagnet, demonstrating that the inorganic network has formed. Attempts to subsequently oxidize the TTF network did not result in stable phases. Iodine vapor oxidation occurred initially, but the film quickly reverted back to the neutral donor form. The result indicates that tethering the organic donors to the inorganic extended network limits their flexibility and therefore hinders the ability of the organic network to reorganize to accommodate the iodide counterions, as is seen in other examples of iodine-doped LB films.

On the other hand, a manganese phosphonate LB film of the donor **42**[203] does form a stable phase when

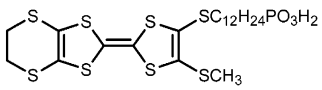

42

photooxidized in the presence of CCl_4 to form a chloride salt following the procedures described by Scott et al.[204] Optical spectroscopy indicates charge delocalization in the organic network. Unfortunately, contact probe conductivity measurements indicated that the film was insulating. AFM images showed that the film was made up of distinct domains approximately 100 nm across that do not percolate over macroscopic distances. Thus, even though spectroscopic evidence suggests the organic network is

conducting, the film topography does not support charge transport. Nevertheless, the example is a step closer to a true dual-network LB film that is both conducting and magnetic.

6. Concluding Remarks

Both conductivity and magnetism have now been achieved in Langmuir–Blodgett films. Not surprisingly, problems inherent to two dimensions plague both areas. In low dimensions, the effects of disruptions in structure are magnified. Defects that break structural or physical property coherence cannot be circumvented. For conducting films, the result is that the macroscopic conductivity is usually lower than the local structure would suggest. For magnetic films, low dimension and limited structural coherence can give rise to glassy behavior. Nevertheless, results to date have significantly advanced our understanding of the factors that govern conductivity and magnetic properties in molecule-based monolayers. More work is needed to improve the quality of the deposited films. Methods of characterization are now readily available that should permit detailed correlations of physical properties with careful determinations of film structure. Careful studies of this nature have been lacking.

Arguably, the most promising future direction is the opportunity to combine properties in a single thin film assembly, as conveyed in the schemes of Figures 1 and 20. Clever combinations of molecular and supramolecular chemistry with LB nanoassembly methods can result in the combinations of properties or new properties not otherwise accessible. These ideas are particularly exciting if molecule-based phenomena can be engineered to combine with typically cooperative solid-state behavior. Efforts in this direction are just beginning.

7. Acknowledgments

I thank Isa O. Benitez for extensive help compiling the figures and chemical structures used in this article and the anonymous reviewers for their many helpful suggestions. Our efforts at the University of Florida in the area of mixed organic/inorganic Langmuir–Blodgett films have often been in collaboration with the group of Professor Mark W. Meisel. I gratefully acknowledge the contributions of Professor Meisel and co-workers from both of our groups. Financial support for the author's work in this area has been provided by the National Science Foundation through Grants DMR-9205333, DMR-9530453, CHE-9618750, and DMR-9900855.

8. References

(1) Parkin, S. S. P.; Engler, E. M.; Lee, V. Y.; Schumaker, R. R. *Mol. Cryst. Liq. Cryst.* **1985**, *119*, 375.
(2) Williams, J. M.; Emge, T. J.; Wang, H. H.; Beno, M. A.; Copps, P. T.; Hall, L. N.; Carlson, K. D.; Crabtree, G. W. *Inorg. Chem.* **1984**, *23*, 2558.
(3) Williams, J. M.; Ferraro, J. R.; Thorn, R. J.; Carlson, K. D.; Geiser, U.; Wang, H. H.; Kini, A. M.; Whangbo, M.-H. *Organic Superconductors*; Simon & Schuster: Englewood Cliffs, NJ, 1992.
(4) Kahn, O. *Molecular Magnetism*; VCH Publishers: New York, 1993.
(5) Cowan, D. O.; Wiygul, F. M. *Chem. Eng. News* **1986**, *28*, 8.
(6) Kahn, O.; Pei, Y.; Nakatani, K.; Journaux, Y.; Sletten, J. *New J. Chem.* **1992**, *16*, 269.
(7) Gaines, G. J. *Insoluble Monolayers at Liquid–Gas Interfaces*; Wiley-Interscience: New York, 1966.
(8) Roberts, G. G. *Langmuir–Blodgett Films*; Plenum Press: New York, 1990.
(9) Ulman, A. *An Introduction to Ultrathin Organic Films: From Langmuir–Blodgett to Self-Assembly*; Academic Press: Boston, 1991.
(10) Petty, M. C. *Langmuir–Blodgett Films. An Introduction*; Cambridge University Press: Cambridge, U.K., 1996.
(11) Barraud, A.; Lessieur, P.; Ruaudel-Teixier, A.; Vandevyver, M. *Thin Solid Films* **1985**, *134*, 195.
(12) Ruaudel-Teixier, A.; Vandevyver, M.; Barraud, A. *Mol. Cryst. Liq. Cryst.* **1985**, *120*, 319.
(13) Delhaes, P.; Yartsev, V. M. In *Spectroscopy of New Materials*; Clark, R. J. H., Hester, R. E., Eds.; John Wiley and Sons: 1993; pp 199–289.
(14) Bryce, M. R.; Petty, M. C. *Nature* **1995**, *374*, 771.
(15) Nakamura, T. In *Handbook of Organic Conductive Molecules and Polymers*; Nalwa, H. S., Ed.; John Wiley and Sons Ltd, 1997; Vol. 1, pp 727–779.
(16) Bjornholm, T.; Hassenkam, T.; Reitzel, N. *J. Mater. Chem.* **1999**, *9*, 1975.
(17) Izumi, M.; Yartsev, V. M.; Ohnuki, H.; Vignau, L.; Delhaes, P. *Recent Res. Dev. Phys. Chem.* **2001**, *5*, 37.
(18) Pomerantz, M.; Pollak, R. A. *Chem. Phys. Lett.* **1975**, *31*, 602.
(19) Pomerantz, M.; Dacol, F. H.; Segmüller, A. *Phys. Rev. Lett.* **1978**, *40*, 246.
(20) Pomerantz, M. *Solid State Commun.* **1978**, *27*, 1413.
(21) Mingotaud, C.; Delhaes, P.; Meisel, M. W.; Talham, D. R. In *Magnetism: Molecules to Materials*; Miller, J. S., Drillon, M., Eds.; Wiley-VCH: New York, 2001; Vol. II, pp 457–484.
(22) Metzger, R. M. *Chem. Rev.* **2003**, *103*, 3803.
(23) Coronado, E.; Mingotaud, C. *Adv. Mater.* **1999**, *11*, 869.
(24) Talham, D. R.; Seip, C. T.; Whipps, S.; Fanucci, G. E.; Petruska, M. A.; Byrd, H. *Comments Inorg. Chem.* **1997**, *19*, 133.
(25) Blodgett, K. B. *J. Am. Chem. Soc.* **1935**, *57*, 1007.
(26) Kuhn, H.; Mobius, D.; Bucher, H. In *Physical Methods of Chemistry*; Weissberger, A., Rossiter, B., Eds.; John Wiley and Sons: 1972; Vol. 1, Part IIIB, pp 577–715.
(27) Lösche, M.; Rabe, J.; Fischer, A.; Rucha, B. U.; Knoll, W.; Mohwald, H. *Thin Solid Films* **1984**, *117*, 269.
(28) Als-Nielsen, J.; Jacquemain, D.; Kjaer, K.; Leveiller, F.; Lahav, M.; Leiserowitz, L. *Phys. Rep.* **1994**, *246*, 252.
(29) Schwartz, D. K.; Garnaes, J.; Viswanathan, R.; Zasadzinski, J. A. N. *Science* **1992**, *257*, 508.
(30) Fanucci, G. E.; Bowers, C. R.; Talham, D. R. *J. Am. Chem. Soc.* **1999**, *121*, 1088.
(31) Byrd, H.; Whipps, S.; Pike, J. K.; Ma, J.; Nagler, S. E.; Talham, D. R. *J. Am. Chem. Soc.* **1994**, *116*, 295.
(32) Pike, J. K.; Byrd, H.; Morrone, A. A.; Talham, D. R. *Chem. Mater.* **1994**, *6*, 1757.
(33) Dhindsa, A. S.; Bryce, M. R.; Ancelin, H.; Petty, M. C.; Yarwood, J. *Langmuir* **1990**, *6*, 1680.
(34) Bertho, F.; Talham, D.; Robert, A.; Batail, P.; Megtert, S.; Robin, P. *Mol. Cryst. Liq. Cryst. Incorporating Nonlinear Opt.* **1988**, *156*, 339.
(35) Barraud, A.; Lequan, M.; Lequan, R. M.; Lesieur, P.; Richard, J.; Ruaudel-Teixier, A.; Vandevyver, M. *J. Chem. Soc., Chem. Commun.* **1987**, 797.
(36) Ruaudel-Teixier, A.; Vandevyver, M.; Roulliay, M.; Bourgoin, J.-P.; Barraud, A.; Lequan, M.; Lequan, R. M. *J. Phys. D: Appl. Phys.* **1990**, *23*, 987.
(37) Kawabata, Y.; Nakamura, T.; Matsumoto, M.; Tanaka, M.; Sekiguchi, T.; Komizu, H.; Manda, E.; Saito, G. *Synth. Met.* **1987**, *19*, 663.
(38) Nakamura, T.; Tanaka, M.; Sekiguchi, T.; Kawabata, Y. *J. Am. Chem. Soc.* **1986**, *108*, 1302.
(39) Jaiswal, A.; Singh, R. A. *Thin Solid Films* **2001**, *394*, 159.
(40) Cea, P.; Artigas, H.; Urieta, J. S.; Lopez, M. C.; Royo, F. M. *J. Colloid Interface Sci.* **2001**, *243*, 156.
(41) Tachibana, H.; Sato, F.; Matsumoto, M. *Thin Solid Films* **2000**, *372*, 237.
(42) Bourgoin, J.-P.; Ruaudel-Teixier, A.; Vandevyver, M.; Roulliay, M.; Barraud, A.; Lequan, M.; Lequan, R.-M. *Makromol. Chem., Macromol. Symp.* **1991**, *46*, 163.
(43) Ikegami, K.; Lan, M.; Nakamura, T. *J. Chem. Phys.* **2000**, *112*, 881.
(44) Ikegami, K.; Lan, M. B.; Nakamura, T. *Synth. Met.* **1999**, *102*, 1615.
(45) Ikegami, K.; Nakamura, T. *Jpn. J. Appl. Phys. Part 2* **1998**, *37*, L550.
(46) Nakamura, T.; Isotalo, H.; Akutagawa, T.; Tachibana, H.; Azumi, R.; Matsumoto, M.; Horiuchi, S.; Yamochi, H.; Saito, G. *Thin Solid Films* **1996**, *285*, 508.

(47) Nakamura, T.; Yunome, G.; Azumi, R.; Tanaka, M.; Tachibana, H.; Matsumoto, M.; Horiuchi, S.; Yamochi, H.; Saito, G. *J. Phys. Chem.* **1994**, *98*, 1882.
(48) Dourthe, C.; Izumi, M.; Garrigou-Lagrange, C.; Buffeteau, T.; Desbat, B.; Delhaes, P. *J. Phys. Chem.* **1992**, *96*, 2812.
(49) Izumi, M.; Dourthe-Lalanne, C.; Dupart, E.; Flandrois, S.; Morand, J.-P.; Delhaes, P. *J. Phys. D: Appl. Phys.* **1991**, *24*, 1141.
(50) Richard, J.; Vandevyver, M.; Barraud, A.; Morand, J. P.; Delhaes, P. *J. Colloid Interface Sci.* **1989**, *129*, 254.
(51) Dhindsa, A. S.; Song, Y.-P.; Badyal, J. P.; Bryce, M. R.; Lvov, Y. M.; Petty, M. C.; Yarwood, J. *Chem. Mater.* **1992**, *4*, 724.
(52) Jia, C. Y.; Zhang, D. Q.; Xu, Y.; Xu, W.; Zhu, D. *Synth. Met.* **2003**, *137*, 979.
(53) Jia, C. Y.; Zhang, D. Q.; Xu, Y.; Xu, W.; Hu, H. M.; Zhu, D. B. *Synth. Met.* **2003**, *132*, 249.
(54) Li, H. X.; Zhang, D. Q.; Xu, Y.; Xu, W.; Yu, G.; Li, X. G.; Zhu, D. B. *Synth. Met.* **2001**, *123*, 385.
(55) Akutagawa, T.; Uchigata, M.; Hasegawa, T.; Nakamura, T.; Nielsen, K. A.; Jeppesen, J. O.; Brimert, T.; Becher, J. *J. Phys. Chem. B* **2003**, *107*, 13929.
(56) Goldenberg, L. M.; Bryce, M. R.; Wegener, S.; Petty, M. C.; Cresswell, J. P.; Lednev, I. K.; Hester, R. E.; Moore, J. N. *J. Mater. Chem.* **1997**, *7*, 2033.
(57) Bryce, M. R.; Moore, A. J.; Batsanov, A. S.; Howard, J. A. K.; Petty, M. C.; Williams, G.; Rotello, V.; Cuello, A. *J. Mater. Chem.* **1999**, *9*, 2973.
(58) Perepichka, D. F.; Bryce, M. R.; Pearson, C.; Petty, M. C.; McInnes, E. J. L.; Zhao, J. P. *Angew. Chem., Int. Ed.* **2003**, *42*, 4636.
(59) Tatewaki, Y.; Akutagawa, T.; Hasegawa, T.; Nakamura, T.; Becher, J. *Synth. Met.* **2003**, *137*, 933.
(60) Akutagawa, T.; Ohta, T.; Hasegawa, T.; Nakamura, T.; Christensen, C. A.; Becher, J. *Proc. Natl. Acad. Sci. U.S.A.* **2002**, *99*, 5028.
(61) Miyata, H.; Tatewaki, Y.; Akutagawa, T.; Hasegawa, T.; Nakamura, T.; Christensen, C. A.; Becher, J. *Thin Solid Films* **2003**, *438*, 1.
(62) Brossard, L.; Ribault, M.; Valade, L.; Cassoux, P. *Physica B & C* **1986**, *143*, 378.
(63) Kobayashi, A.; Suzuki, W. *Mol. Cryst. Liq. Cryst.* **2002**, *380*, 37.
(64) Nakamura, T.; Tanaka, H.; Kojima, K.; Matsumoto, M.; Tachibana, H.; Tanaka, M.; Kawabata, Y. *Thin Solid Films* **1989**, *179*, 183.
(65) Nakamura, T.; Kojima, K.; Matsumoto, M.; Tachibana, H.; Tanaka, M.; Manda, E.; Kawabata, Y. *Chem. Lett.* **1989**, 367.
(66) Matsuzaki, H.; Ogasawara, K.; Ishiguro, T.; Nogami, Y.; Taoda, M.; Tachibana, H.; Matsumoto, M.; Nakamura, T. *Synth. Met.* **1995**, *74*, 251.
(67) Dhindsa, A. S.; Badyal, J. P.; Pearson, C.; Bryce, M. R.; Petty, M. C. *J. Chem. Soc., Chem. Commun.* **1991**, 322.
(68) Miura, Y. F.; Horikiri, M.; Saito, S. H.; Sugi, M. *Solid State Commun.* **2000**, *113*, 603.
(69) Miura, Y. F.; Horikiri, M.; Tajima, S.; Wakaita, T.; Saito, S.-H.; Sugi, M. *Synth. Met.* **2003**, *133*−*134*, 663.
(70) Miura, Y. F.; Hedo, M.; Uwatoko, Y.; Saito, S.-H.; Sugi, M. *Synth. Met.* **2003**, *137*, 1311.
(71) Horikiri, M.; Miura, Y. F.; Okuma, Y.; Ikegami, K.; Sugi, M. *Jpn. J. Appl. Phys. Part 1* **2001**, *40*, 295.
(72) Horikiri, M.; Miura, Y. F.; Araki, Y.; Ikegami, K.; Sugi, M. *Colloids Surf. A: Physicochem. Eng. Aspects* **2002**, *198*, 657.
(73) Horikiri, M.; Araki, Y.; Ikegami, K.; Miura, Y. F.; Sugi, M. *Synth. Met.* **2003**, *133*, 665.
(74) Xu, Y.; Li, H. Q.; Liu, Y. Q.; Tan, G. Z.; Zhu, D. B.; Yu, X. D. *Thin Solid Films* **2000**, *375*, 251.
(75) Takahashi, T.; Sakai, K.; Yumoto, T.; Akutagawa, T.; Hasegawa, T.; Nakamura, T. *Thin Solid Films* **2001**, *393*, 7.
(76) Nakamura, T.; Takahashi, T.; Yumoto, T.; Akutagawa, T.; Hasegawa, T. *Chem. Lett.* **2001**, 134.
(77) Ohnuki, H.; Desbat, B.; Giffard, M.; Izumi, M.; Imakubo, T.; Mabon, G.; Delhaes, P. *J. Phys. Chem. B* **2001**, *105*, 4921.
(78) Ohnuki, H.; Ishizaki, Y.; Suzuki, M.; Desbat, B.; Delhaes, P.; Giffard, M.; Imakubo, T.; Mabon, G.; Izumi, M. *Materials Science & Engineering C*−*Biomimetic and Supramolecular Systems* **2002**, *22*, 227.
(79) Ishizaki, Y.; Suzuki, M.; Ohnuki, H.; Imakubo, T.; Izumi, M. *Synth. Met.* **2003**, *133*, 669.
(80) Ishizaki, Y.; Izumi, M.; Ohnuki, H.; Imakubo, T.; Kalita-Lipinska, K. *Colloids Surf. A: Physicochem. Eng. Aspects* **2002**, *198*, 723.
(81) Ishizaki, Y.; Izumi, M.; Ohnuki, H.; Kalita-Lipinska, K.; Imakubo, T.; Kobayashi, K. *Phys. Rev. B* **2001**, *6313*.
(82) Ohnuki, H.; Suzuki, M.; Ishizaki, Y.; Imakubo, T.; Ida, T.; Izumi, M. *Synth. Met.* **2003**, *137*, 927.
(83) Ohnuki, H.; Nagata, M.; Ishizaki, Y.; Imakubo, T.; Kobayashi, K.; Kato, R.; Izumi, M. *Synth. Met.* **1999**, *102*, 1699.
(84) Ishizaki, Y.; Ida, T.; Yartsev, V. M.; Ohnuki, H.; Imakubo, T.; Izumi, M. *Synth. Met.* **2003**, *137*, 925.
(85) Granito, C.; Goldenberg, L. M.; Bryce, M. R.; Monkman, A. P.; Troisi, L.; Pasimeni, L.; Petty, M. C. *Langmuir* **1996**, *12*, 472.
(86) Gregory, B. W.; Vaknin, D.; Gray, J. D.; Ocko, B. M.; Stroeve, P.; Cotton, T. M.; Struve, W. S. *J. Phys. Chem. B* **1997**, *101*, 2006.
(87) Armstrong, N. R. *J. Porphyrins Phthalocyanines* **2000**, *4*, 414.
(88) Donley, C. L.; Xia, W.; Minch, B. A.; Zangmeister, R. A. P.; Drager, A. S.; Nebesny, K.; O'Brien, D. F.; Armstrong, N. R. *Langmuir* **2003**, *19*, 6512.
(89) Drager, A. S.; Zangmeister, R. A. P.; Armstrong, N. R.; O'Brien, D. F. *J. Am. Chem. Soc.* **2001**, *123*, 3595.
(90) Smolenyak, P. E.; Osburn, E. J.; Chen, S. Y.; Chau, L. K.; O'Brien, D. F.; Armstrong, N. R. *Langmuir* **1997**, *13*, 6568.
(91) Smolenyak, P.; Peterson, R.; Nebesny, K.; Torker, M.; O'Brien, D. F.; Armstrong, N. R. *J. Am. Chem. Soc.* **1999**, *121*, 8628.
(92) Zangmeister, R. A. P.; Smolenyak, P. E.; Drager, A. S.; O'Brien, D. F.; Armstrong, N. R. *Langmuir* **2001**, *17*, 7071.
(93) Xia, W.; Minch, B. A.; Carducci, M. D.; Armstrong, N. R. *Langmuir* **2004**, *20*, 7998.
(94) Donley, C. L.; Zangmeister, R. A. P.; Xia, W.; Minch, B. A.; Drager, A. S.; Cherian, S. K.; LaRussa, L.; Kippelen, B.; Domercq, B.; Mathine, D. L.; O'Brien, D. F.; Armstrong, N. R. *J. Mater. Res.* **2004**, *19*, 2087.
(95) Vandevyver, M. *Thin Solid Films* **1992**, *210*, 240.
(96) Richard, J.; Vandevyver, M.; Lesieur, P.; Barraud, A.; Holczer, K. *J. Phys. D: Appl. Phys.* **1986**, *19*, 2421.
(97) Pearson, C.; Dhindsa, A. S.; Bryce, M. R.; Petty, M. C. *Supramol. Sci.* **1997**, *4*, 443.
(98) Galchenkov, L. A.; Ivanov, S. N.; Pyataikin, II.; Chernov, V. P. *Solid State Commun.* **2003**, *127*, 577.
(99) Troitsky, V. I.; Berzina, T. S.; Fontana, M. P. *Colloids Surf. A: Physicochem. Eng. Aspects* **2002**, *198*, 689.
(100) Pradeau, J. P.; Perez, H.; Armand, F. *J. Phys. D: Appl. Phys.* **1999**, *32*, 961.
(101) Reitzel, N.; Greve, D. R.; Kjaer, K.; Hows, P. B.; Jayaraman, M.; Savoy, S.; McCullough, R. D.; McDevitt, J. T.; Bjornholm, T. *J. Am. Chem. Soc.* **2000**, *122*, 5788.
(102) Pomerantz, M. In *NATO ASI Series*—*Phase Transitions in Surface Films*; Dash, J. G., Ruvalds, J., Eds.; Plenum Press: New York, 1980; pp 317−346.
(103) Pomerantz, M. *Surf. Sci.* **1984**, *142*, 556.
(104) Bonosi, F.; Gabrielli, G.; Martini, G. *Colloids Surf. A: Physicochem. Eng. Aspects* **1993**, *72*, 105.
(105) Takamura, T.; Matsushita, K.; Shimoyama, Y. *Jpn. J. Appl. Phys. Part 1* **1996**, *35*, 5831.
(106) Hutchison, W. D.; Clark, R. G.; Yazidjoglou, N.; Jamie, I. M.; Chaplin, D. H.; Creagh, D. C. *Solid State Commun.* **1999**, *109*, 239.
(107) Haseda, T.; Yamakawa, H.; Ishizuka, M.; Okuda, Y.; Kubota, T.; Hata, M.; Amaya, K. *Solid State Commun.* **1977**, *24*, 599.
(108) Drillon, M.; Panissod, P. *J. Magn. Magn. Mater.* **1998**, *188*, 93.
(109) Bloch, F. *Z. Phys.* **1930**, *61*, 206.
(110) Mermin, N. D.; Wagner, H. *Phys. Rev. Lett.* **1966**, *17*, 1133.
(111) Tyutyulkov, N.; Ivanova, A.; Dietz, F. *Chem. Phys.* **2003**, *287*, 71.
(112) Tyutyulkov, N.; Staykov, A.; Mullen, K.; Dietz, F. *Langmuir* **2002**, *18*, 10030.
(113) Carmeli, I.; Leitus, G.; Naaman, R.; Reich, S.; Vager, Z. *J. Chem. Phys.* **2003**, *118*, 10372.
(114) Ivanov, B. A.; Tartakovskaya, E. V. *JETP Lett.* **1996**, *63*, 835.
(115) Volkel, A. R.; Mertens, F. G.; Bishop, A. R.; Wysin, G. M. *Ann. Phys.* **1993**, *2*, 308.
(116) Ando, Y.; Hiroike, T.; Miyashita, T.; Miyazaki, T. *Thin Solid Films* **1995**, *266*, 292.
(117) Ando, Y.; Hiroike, T.; Miyashita, T.; Miyazaki, T. *Thin Solid Films* **1996**, *278*, 144.
(118) Giesse, E.; Dengler, J.; Ritter, G.; Wagner, W.; Brandl, D.; Voit, H.; Saemannischenko, G. *Solid State Commun.* **1993**, *86*, 243.
(119) Giesse, E.; Dengler, J.; Ritter, G.; Brandl, D.; Voit, H. *Hyperfine Interact.* **1994**, *93*, 1415.
(120) Giesse, E.; Ritter, G.; Brandl, D.; Voit, H.; Rozlosnik, N. *Hyperfine Interact.* **1995**, *95*, 175.
(121) Tishin, A. M.; Koksharov, Y. A.; Bohr, J.; Khomutov, G. B. *Phys. Rev. B* **1997**, *55*, 11064.
(122) Koksharov, Y. A.; Bykov, I. V.; Malakho, A. P.; Polyakov, S. N.; Khomutov, G. B.; Bohr, J. *Mater. Sci. Eng. C: Biomimetic Supramol. Syst.* **2002**, *22*, 201.
(123) Tishin, A. M.; Snigirev, O. V.; Khomutov, G. B.; Gudoshnikov, S. A.; Bohr, J. *J. Magn. Magn. Mater.* **2001**, *234*, 499.
(124) Khomutov, G. B.; Koksharov, Y. A.; Radchenko, I. L.; Soldatov, E. S.; Trifonov, A. S.; Tishin, A. M.; Bohr, J. *Mater. Sci. Eng. C: Biomimetic Supramol. Syst.* **1999**, *8*−*9*, 299.
(125) Aktsipetrov, O. A.; Didenko, N. V.; Fedyanin, A. A.; Khomutov, G. B.; Murzina, T. V. *Mater. Sci. Eng. C: Biomimetic Supramol. Syst.* **1999**, *8*−*9*, 411.
(126) Mukhopadhyay, M. K.; Sanyal, M. K.; Mukadam, M. D.; Yusuf, S. M.; Basu, J. K. *Phys. Rev. B* **2003**, *68*, 174427/1.
(127) Byrd, H.; Pike, J. K.; Talham, D. R. *Synth. Met.* **1995**, *71*, 1977.

(128) Seip, C. T.; Granroth, G. E.; Meisel, M. W.; Talham, D. R. *J. Am. Chem. Soc.* **1997**, *119*, 7084.
(129) Byrd, H.; Pike, J. K.; Talham, D. R. *Chem. Mater.* **1993**, *5*, 709.
(130) Seip, C. T.; Talham, D. R. *Mater. Res. Bull.* **1999**, *34*, 437.
(131) Fanucci, G. E.; Talham, D. R. *Langmuir* **1999**, *15*, 3289.
(132) Byrd, H.; Pike, J. K.; Talham, D. R. *J. Am. Chem. Soc.* **1994**, *116*, 7903.
(133) Fanucci, G. E.; Petruska, M. A.; Meisel, M. W.; Talham, D. R. *J. Solid State Chem.* **1999**, *145*, 443.
(134) Petruska, M. A.; Watson, B. C.; Meisel, M. W.; Talham, D. R. *Chem. Mater.* **2002**, *14*, 2011.
(135) Petruska, M. A.; Watson, B. C.; Meisel, M. W.; Talham, D. R. *Mol. Cryst. Liq. Cryst.* **2002**, *376*, 121.
(136) Seip, C. T.; Byrd, H.; Talham, D. R. *Inorg. Chem.* **1996**, *35*, 3479.
(137) Fanucci, G. E.; Krzystek, J.; Meisel, M. W.; Brunel, L.-C.; Talham, D. R. *J. Am. Chem. Soc.* **1998**, *120*, 5469
(138) Cao, G.; Lee, H.; Lynch, V. M.; Mallouk, T. E. *Inorg. Chem.* **1988**, *27*, 2781.
(139) Carling, S. G.; Day, P.; Visser, D.; Kremer, R. K. *J. Solid State Chem.* **1993**, *106*, 111.
(140) Carling, S. G.; Day, P.; Visser, D. *Inorg. Chem.* **1995**, *34*, 3917.
(141) Culp, J. T.; Davidson, M.; Duran, R. S.; Talham, D. R. *Langmuir* **2002**, *18*, 8260.
(142) Gadet, V.; Mallah, T.; Castro, I.; Verdaguer, M.; Veillet, P. *J. Am. Chem. Soc.* **1992**, *114*, 9213.
(143) Mallah, T.; Thiebaut, S.; Verdaguer, M.; Veillet, P. *Science* **1993**, *262*, 1554.
(144) Ently, W. R.; Girolami, G. S. *Science* **1995**, *268*, 397.
(145) Ently, W. R.; Girolami, G. S. *Inorg. Chem.* **1994**, *33*, 5165.
(146) Verdaguer, M.; Bleuzen, A.; Marvaud, V.; Vaissermann, J.; Seuleiman, M.; Desplanches, C.; Scuiller, A.; Train, C.; Garde, R.; Gelly, G.; Lomenech, C.; Rosenman, I.; Veillet, P.; Cartier, C.; Villain, F. *Coord. Chem. Rev.* **1999**, *192*, 1023.
(147) Mallah, T.; Auberger, C.; Verdaguer, M.; Veillet, P. *J. Chem. Soc., Chem. Commun.* **1995**, 61.
(148) Scuiller, A.; Mallah, T.; Verdaguer, M.; Nivorozkhin, A.; Tholence, J. L.; Veillet, P. *New J. Chem.* **1996**, *20*, 1.
(149) Parker, R. J.; Spiccia, L.; Berry, K. J.; Fallon, G. D.; Moubaraki, B.; Murray, K. S. *J. Chem. Soc., Chem. Commun.* **2001**, 333.
(150) Larionova, J.; Gross, M.; Pilkington, M.; Andres, H.; Stoeckli-Evans, H.; Gudel, H. U.; Decurtins, S. *Angew. Chem., Int. Ed.* **2000**, *39*, 1605.
(151) Shores, M. P.; Sokol, J. J.; Long, J. R. *J. Am. Chem. Soc.* **2002**, *124*, 2279.
(152) Berseth, P. A.; Sokol, J. J.; Shores, M. P.; Heinrich, J. L.; Long, J. R. *J. Am. Chem. Soc.* **2000**, *122*, 9655.
(153) Ohba, M.; Okawa, H. *Coord. Chem. Rev.* **2000**, *198*, 313.
(154) Marvilliers, A.; Parsons, S.; Riviere, E.; Audiere, J. P.; Kurmoo, M.; Mallah, T. *Eur. J. Inorg. Chem.* **2001**, 1287.
(155) Kou, H. Z.; Bu, W. M.; Liao, D. Z.; Jiang, Z. H.; Yan, S. P.; Fan, Y. G.; Wang, G. L. *J. Chem. Soc., Dalton Trans.* **1998**, 4161.
(156) Holmes, S. M.; Girolami, G. S. *J. Am. Chem. Soc.* **1999**, *121*, 5593.
(157) Hatlevik, O.; Buschmann, W. E.; Zhang, J.; Manson, J. L.; Miller, J. S. *Adv. Mater.* **1999**, *11*, 914.
(158) Ferlay, S.; Mallah, T.; Ouahes, R.; Veillet, P.; Verdaguer, M. *Nature* **1995**, *378*, 701.
(159) Buschmann, W. E.; Miller, J. S. *Inorg. Chem.* **2000**, *39*, 2411.
(160) Buschmann, W. E.; Ensling, J.; Gutlich, P.; Miller, J. S. *Chem.–Eur. J.* **1999**, *5*, 3019.
(161) Shimamoto, N.; Ohkoshi, S.; Sato, O.; Hashimoto, K. *Inorg. Chem.* **2002**, *41*, 678.
(162) Escax, V.; Bleuzen, A.; Moulin, C. C. D.; Villain, F.; Goujon, A.; Varret, F.; Verdaguer, M. *J. Am. Chem. Soc.* **2001**, *123*, 12536.
(163) Sato, O.; Iyoda, T.; Fujishima, A.; Hashimoto, K. *Science* **1996**, *272*, 704.
(164) Mingotaud, C.; Lafuente, C.; Gomez-Garcia, C.; Ravaine, S.; Delhaes, P. *Mol. Cryst. Liq. Cryst. Sci. Technol. A* **1999**, *335*, 1061.
(165) Mingotaud, C.; Lafuente, C.; Amiell, J.; Delhaes, P. *Langmuir* **1999**, *15*, 289.
(166) Lafuente, C.; Mingotaud, C.; Delhaes, P. *Chem. Phys. Lett.* **1999**, *302*, 523.
(167) Romualdo-Torres, G.; Agricole, B.; Mingotaud, C.; Ravaine, S.; Delhaes, P. *Langmuir* **2003**, *19*, 4688.
(168) Culp, J. T.; Park, J. H.; Stratakis, D.; Meisel, M. W.; Talham, D. R. *J. Am. Chem. Soc.* **2002**, *124*, 10083.
(169) Culp, J. T.; Park, J. H.; Meisel, M. W.; Talham, D. R. *Polyhedron* **2003**, *22*, 3059.
(170) Culp, J. T.; Park, J. H.; Meisel, M. W.; Talham, D. R. *Inorg. Chem.* **2003**, *42*, 2842.
(171) Park, J. H.; Culp, J. T.; Hall, D. W.; Talham, D. R.; Meisel, M. W. *Physica B: Condens. Matter* **2003**, *329*, 1152.
(172) Rabu, P.; Drillon, M. *Adv. Eng. Mater.* **2003**, *5*, 189.
(173) Kuroda, S. *Colloids Surf. A: Physicochem. Eng. Aspects* **1993**, *72*, 127.
(174) Le Moigne, J.; Gallani, J. L.; Wautelet, P.; Moroni, M.; Oswald, L.; Cruz, C.; Galerne, Y.; Arnault, J. C.; Duran, R.; Garrett, M. *Langmuir* **1998**, *14*, 7484.
(175) Gallani, J. L.; Le Moigne, J.; Oswald, L.; Bernard, M.; Turek, P. *Langmuir* **2001**, *17*, 1104.
(176) Bai, C.; Zhang, P.; Zhu, D.; Han, M.; Xu, Y.; Zhang, D.; Liu, Y. *J. Phys. Chem.* **1995**, *99*, 8202.
(177) Xu, Y.; Zhang, D. Q.; Zhang, P. C.; Liu, Y. Q.; Han, M. Y.; Zhu, D. B. *Thin Solid Films* **1996**, *285*, 537.
(178) Zhang, D. Q.; Ding, L.; Xu, Y.; Zhu, D. B. *Chin. Chem. Lett.* **1999**, *10*, 0, 685.
(179) Clemente-León, M.; Mingotaud, C.; Agricole, B.; Gómez-Garcia, C. J.; Coronado, E.; Delhaes, P. *Angew. Chem., Int. Ed.* **1997**, *36*, 1114.
(180) Clemente-León, M.; Mingotaud, C.; Gómez-Garcia, C. J.; Coronado, E.; Delhaes, P. *Thin Solid Films* **1998**, *329*, 439.
(181) Clemente-León, M.; Agricole, B.; Mingotaud, C.; Gómez-Garcia, C.; Coronado, E.; Delhaes, P. *Langmuir* **1997**, *13*, 2340.
(182) Mathoniere, C.; Nuttall, C. J.; Carling, S. G.; Day, P. *Inorg. Chem.* **1996**, *35*, 1201.
(183) Decurtins, S.; Schmalle, H. W.; Oswald, H. R.; Linden, A.; Ensling, J.; Gutlich, P.; Hauser, A. *Inorg. Chim. Acta* **1994**, *216*, 65.
(184) Tamaki, H.; Zhong, Z. J.; Matsumoto, N.; Kida, S.; Koikawa, M.; Achiwa, N.; Hashimoto, Y.; Okawa, H. *J. Am. Chem. Soc.* **1992**, *114*, 6974.
(185) Aiai, M.; Ramos, J.; Mingotaud, C.; Amiell, J.; Delhaes, P.; Jaiswal, A.; Singh, R. A.; Singh, B.; Singh, B. P. *Chem. Mater.* **1998**, *10*, 728.
(186) Clemente-León, M.; Soyer, H.; Mingotaud, C.; Gómez-Garcia, C. J.; Coronado, E.; Delhaes, P. *Synth. Met.* **1999**, *103*, 2263.
(187) Clemente-León, M.; Coronado, E.; Forment-Aliaga, A.; Romero, F. M. *C. R. Chim.* **2003**, *6*, 683.
(188) Clemente-León, M.; Soyer, H.; Coronado, E.; Mingotaud, C.; Gómez-Garcia, C. J.; Delhaes, P. *Angew. Chem., Int. Ed.* **1998**, *37*, 2842.
(189) Sessoli, R.; Tsai, H. L.; Schake, A. R.; Wang, S. Y.; Vincent, J. B.; Folting, K.; Gatteschi, D.; Christou, G.; Hendrickson, D. N. *J. Am. Chem. Soc.* **1993**, *115*, 1804.
(190) Vaknin, D.; Miller, L. L.; Eshel, M.; Bino, A. *J. Phys. Chem. B* **2001**, *105*, 8014.
(191) Gutlich, P.; Hauser, A.; Spiering, H. *Angew. Chem., Int. Ed. Engl.* **1994**, *33*, 2024.
(192) Kahn, O.; Kröber, J.; Jay, C. *Adv. Mater.* **1992**, *4*, 718.
(193) Ruaudel-Teixier, A.; Barraud, A.; Coronel, P.; Kahn, O. *Thin Solid Films* **1988**, *160*, 107.
(194) Armand, F.; Badoux, C.; Bonville, P.; Ruaudel-Teixier, A.; Kahn, O. *Langmuir* **1995**, *11*, 3467.
(195) Soyer, H.; Dupart, E.; Mingotaud, C.; Gomez-Garcia, C.; Delhaès, P. *Colloids Surf. A: Phys. Eng. Aspects* **2000**, *171*, 275.
(196) Soyer, H.; Mingotaud, C.; Boillot, M. L.; Delhaes, P. *Langmuir* **1998**, *14*, 5890.
(197) Soyer, H.; Dupart, E.; Gomez-Garcia, C. J.; Mingotaud, C.; Delhaes, P. *Adv. Mater.* **1999**, *11*, 382.
(198) Letard, J. F.; Nguyen, O.; Soyer, H.; Mingotaud, C.; Delhaes, P.; Kahn, O. *Inorg. Chem.* **1999**, *38*, 3020.
(199) Talham, D. R.; Seip, C. T.; Whipps, S.; Fanucci, G. E.; Petruska, M. A.; Byrd, H. *Comments Inorg. Chem.* **1997**, *19*, 133.
(200) Petruska, M. A.; Talham, D. R. *Chem. Mater.* **1998**, *10*, 3673.
(201) Rumualdo-Torres, G.; Dupart, E.; Mingotaud, C.; Ravaine, S. *J. Phys. Chem. B* **2000**, *104*, 9487.
(202) Clemente-León, M.; Coronado, E.; Delhaes, P.; Gómez-Garcia, C. J.; Mingotaud, C. *Adv. Mater.* **2001**, *13*, 574.
(203) Petruska, M. A. Ph.D. Thesis, University of Florida, Gainesville, FL, 2000; p 258.
(204) Scott, B. A.; Kaufman, F. B.; Engler, E. M. *J. Am. Chem. Soc.* **1976**, *98*, 4342.

CR030665U